CME

Zonisamide improves motor function in Parkinson disease

A randomized, double-blind study

Miho Murata, MD, PhD; Kazuko Hasegawa, MD, PhD; Ichiro Kanazawa, MD, PhD; and The Japan Zonisamide on PD Study Group*

Abstract—*Objective:* To evaluate the efficacy, safety and tolerability of daily doses of 25, 50, and 100 mg of zonisamide (ZNS) administered as adjunctive treatment in patients with Parkinson disease (PD). *Methods:* We conducted a multicenter, randomized, double-blind, parallel-treatment, placebo-controlled study in Japan. Patients with PD who showed insufficient response to levodopa treatment were given placebo for 2 weeks and then treated for 12 weeks with 25, 50, or 100 mg/day of ZNS or placebo, in addition to levodopa, followed by a 2-week dose-reduction period. The primary endpoint was change from baseline in the total score of the Unified Parkinson's Disease Rating Scale (UPDRS) Part III at the final assessment point. Secondary endpoints included changes from baseline in total daily "off" time; total scores of UPDRS Parts I, II, and IV; and Modified Hoehn and Yahr Scale score. Safety analysis was based on the incidence of adverse events. *Results:* There was significant improvement in the primary endpoint in the 25-mg and 50-mg groups *vs* placebo. The duration of "off" time was significantly reduced in the 50-mg and 100-mg groups *vs* placebo. Dyskinesia was not increased in ZNS groups. The incidence of adverse effects was similar between the 25-mg, 50-mg, and placebo groups but higher in the 100-mg group. *Conclusions:* Zonisamide is safe, effective and well tolerated at 25 to 100 mg/day as an adjunctive treatment in patients with Parkinson disease.

NEUROLOGY 2007;68:45–50

Zonisamide (ZNS) (1,2-benzisoxazole-3-methanesulfonamide) is an antiepileptic drug with a long-half life ($T_{1/2}$ = 62 hours) that was originally synthesized in Japan.[1] ZNS has been used to treat epilepsy in Japan for more than 10 years; is currently approved for marketing in the United States, Europe, and Korea; and is generally well tolerated. We reported previously that ZNS has beneficial effects on PD in one patient with convulsion attacks.[2] Based on this finding, we subsequently performed an open trial in nine patients with PD and found that ZNS improved the main symptoms of PD, with particular benefits on motor fluctuation, known as "wearing-off."[2] Then, we conducted a small double-blind study that showed a daily dose of 50 to 100 mg of ZNS as an adjunct therapy significantly improved limb rigidity, tremor, and postural instability in patients with advanced PD and was well tolerated.[3]

In this study, we sought to confirm ZNS effectiveness as an adjunctive treatment for PD by evaluating the efficacy, safety, and tolerability of daily oral doses of 25, 50, and 100 mg of ZNS (once a day) in a large population of patients with PD who showed insufficient response to levodopa treatment.

Additional material related to this article can be found on the *Neurology* Web site. Go to www.neurology.org and scroll down the Table of Contents for the January 2 issue to find the title link for this article.

Methods. This was a multicenter, randomized, double-blind, parallel-treatment, placebo-controlled study of ZNS as adjunctive treatment in patients with PD who showed insufficient response to levodopa (including dopa decarboxylase inhibitor: DCI combination drugs). Fifty-eight institutions throughout Japan participated in the study during the study period of January 15 to December 1, 2004.

Patients with PD of both sexes between ages 20 and 80 years were enrolled in the study. Patients who exhibited any problems based on levodopa therapy, such as wearing-off phenomena, "on"–"off" phenomena, and freezing phenomena, no-"on" and delayed-"on," or in whom the suboptimal dose of levodopa had been administered because of side effects or therapeutic strategy were not excluded from the study. Patients had received individual dosages of levodopa (plus a DCI) and were stable for at least 28 days before study initiation. Patients who fulfilled the above criteria were enrolled into the study by the investigators at each participating institution. Patients who met the above criteria and provided informed consent were randomized into the treatment groups of 25, 50, or 100 mg/day ZNS or placebo.

The study consisted of a 2-week run-in period of single-blind treatment with placebo, a 12-week double-blind treatment period, and a 2-week double-blind dose-reduction period (figure E-1 on the Neurology Web site at www.neurology.org), with the exception

*See the appendix for a full list of study participants.

From the Department of Neurology (M.M., I.K.), Musashi Hospital, National Center of Neurology and Psychiatry, Tokyo, Japan; and Division of Neurology (K.H.), Sagamihara Hospital, Kanagawa, Japan.

Disclosure: Sponsored by Dainippon Sumitomo Pharma. All authors have agreed to the conditions noted on the Author Disclosure Form.

Received January 6, 2006. Accepted in final form September 25, 2006.

Address correspondence and reprint requests to Dr. Miho Murata, Department of Neurology, Musashi Hospital, National Center of Neurology and Psychiatry, 4-1-1 Ogawahigashimachi, Kodaira, Tokyo 187-8551, Japan; e-mail: mihom@ncnp.go.jp

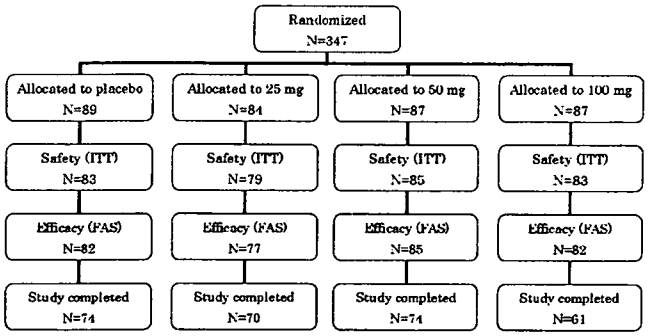

Figure 1. Patient disposition. ITT = intent-to-treat; FAS = full analysis set.

that the 25-mg group did not undergo dose reduction. Baseline assessment was conducted after a 2-week run-in period to reduce placebo effects. Clinical assessment including the Unified Parkinson's Disease Rating Scale (UPDRS) and Hoehn and Yahr staging was conducted at "on" state every 2 weeks.

The daily dosage was administered orally once a day in the morning as four tablets in the run-in and treatment periods and two tablets in the dose-reduction period. Study medication was dispensed as ZNS 25 mg tablets or matching placebo. Patients were randomized to one of the four treatment groups in blocks of size 8 (2 patients per group) during the run-in period using a randomization code generated by the study sponsor or designee. Study medication, indistinguishable by appearance, packaging, and labeling, was provided to each institution, and 1-week supplies were dispensed to patients according to the randomization code.

Patients were required to have concomitant administration with levodopa preparations including DCI combination drugs and were allowed to continue with other anti-Parkinson medications, such as dopamine receptor agonists (DAs), monoamine oxidase type B (MAO-B) inhibitors, anticholinergics, amantadine, or droxydopa, during the study. The dose regimens of these concomitant medications were to be maintained from 4 weeks before study initiation until the end of the dose-reduction period, except as required to alleviate dyskinesia or psychotic symptoms that were likely caused by dopaminergic-receptor hyperstimulation due to concomitant medication.

The primary endpoint was a change from baseline in the total score of UPDRS Part III (motor examination score) at the final assessment point. Secondary endpoints included a change from baseline in total daily "off" time as determined from patients' diaries, and changes from baseline in UPDRS Part I, II, and IV scores and Modified Hoehn and Yahr Scale score. Changes from baseline at the assessment point were analyzed by analysis of covariance using treatment group as a factor, and baseline value and treatment group scores were compared with placebo using the Dunnett test. A significance level of 0.05 (two-sided) was used for intergroup comparison, except for homogeneity assessment, when a significance level of 0.15 (two-sided) was used. The planned sample size of 80 patients per group (320 patients in total) was selected based on a requirement of 69 patients per group to achieve 80% power for comparison between placebo and each of the ZNS groups, assuming a between-group difference of 5.5 and an SD of 10.0 on the primary endpoint as seen in a preliminary study.[3] Multiplicity was taken into consideration in the primary analysis, but not in the secondary analysis or assessment of the dose–response relationship. Subgroup subset analysis was performed for the primary endpoint. Safety assessment was based on the incidence of adverse events including abnormalities of clinical/laboratory examinations and the incidence compared between the treatment groups by χ^2 test. Demographic and efficacy analyses were performed on the full analysis set (FAS), and safety assessments were performed on the intent-to-treat (ITT) population.

Results. Patient disposition is summarized in figure 1. Of the 347 screened and randomized patients, 279 patients (80.4%) completed the protocol as planned. There were no major differences between groups except that markedly fewer patients in the ZNS 100 mg group completed the study. The ITT population consisted of 330 patients (95.1%), with 83 patients in the placebo group, 79 in the 25-mg group, 85 in the 50-mg group, and 83 in the 100-mg group. A total of 6 patients in the placebo group, 5 in the 25-mg group, 2 in the 50-mg group, and 4 in the 100-mg group were not included in the ITT population because of withdrawal of consent or dosing regimen violation. The FAS consisted of the ITT minus 4 patients: 2 in the 25-mg group and 1 in each of the placebo and 100-mg groups because of no efficacy data during and after treatment period. Of the 326 patients (FAS), 279 patients completed the therapy period, and 47 patients discontinued therapy prematurely (8 patients in the placebo group, 7 in the 25-mg group, 11 in the 50-mg group, and 21 in the 100-mg group). The most common reason for discontinuation was adverse events (4 patients in the placebo group, 5 in the 25-mg group, 4 in the 50-mg group, and 9 in the 100-mg group). There were no Good Clinical Practice deviations in this study.

Table 1 shows the demographic background of patients in the placebo and ZNS treatment groups. There were no major differences between groups with respect to patients' background, including disease and treatment histories. The mean morbidity period was 8.6 years, and the mean modified Hoehn and Yahr Scale score ("on") was 2.5. The mean number of concomitant anti-Parkinson medicines was 3.2. The most common concomitant medications were DAs, which were used by 91.7% of the patients, and MAO-B inhibitors, which were used by 51.5% of the patients.

The changes (least-squares mean ± SE) in UPDRS Part III total score from baseline at final assessment were as follows: placebo group, −2.0 ± 0.8; 25-mg group, −6.3 ± 0.8; 50-mg group, −5.8 ± 0.8; and 100-mg group, −4.6 ± 0.8 (figure 2). All treatment groups showed decreases of UPDRS Part III total scores from baseline, but the improvement was significant for the 25-mg ($p = 0.001$, Dunnett test) and 50-mg ($p = 0.003$, Dunnett test) groups, vs the placebo group.

The proportions of responders, defined as patients with ≥30% reduction in UPDRS Part III total score from baseline at final assessment, were as follows: placebo group, 22.0% (18/82); 25-mg group, 35.1% (27/77, $p = 0.067$, χ^2 test vs placebo group); 50-mg group, 38.8% (33/85, $p = 0.018$, χ^2 test vs placebo group); and 100-mg group, 31.7% (26/82, $p = 0.158$, χ^2 test vs placebo group).

The degree of change for the primary endpoint were similar in the 25-mg and 50-mg groups, and these were greater than in the 100-mg group and significantly greater than in the placebo group. Subgroup analyses indicated no significant effects in subject baseline characteristics including with or without MAO-B inhibitor (table E-1) on the primary endpoint.

The mean decrease in total "off" time from baseline at final assessment is shown in figure 3. The mean changes in "off" time (hours) from baseline were as follows: placebo group, −0.20 (n = 61); 25-mg group, −0.22 (n = 58); 50-mg group, −1.30 (n = 68); and 100-mg group, −1.63 (n = 52). The duration of daily "off" time decreased for all treatment groups with improvement in the 50-mg ($p = 0.014$, Dunnett test) and 100-mg ($p = 0.013$, Dunnett test) groups compared with the placebo group.

Table 1 Demographic and baseline characteristics of patients according to the dose of zonisamide

		ZNS		
	Placebo	25 mg/day	50 mg/day	100 mg/day
n	82	77	85	82
Age, years	65.3 (7.5)	65.1 (8.5)	63.9 (9.4)	65.7 (8.6)
Older than 65 years	47 (57.3%)	42 (54.5%)	46 (54.1%)	53 (64.6%)
Men	41 (50.0%)	42 (54.5%)	51 (60.0%)	47 (57.3%)
Duration of PD, years	8.9 (5.8)	8.5 (4.6)	8.6 (6.0)	8.5 (5.6)
Dose of l-dopa, mg/day	351.2 (138.8)	355.5 (115.6)	363.9 (177.4)	327.7 (118.2)
Wearing-off	67 (81.7%)	64 (83.1%)	74 (87.1%)	62 (75.6%)
Dyskinesia	28 (34.1%)	18 (23.4%)	33 (38.8%)	22 (26.8%)
+ Dopamine agonist	80 (97.6%)	76 (98.7%)	85 (100.0%)	80 (97.6%)
+ MAO-B inhibitor	42 (51.2%)	38 (49.4%)	43 (50.6%)	45 (54.9%)
UPDRS Part III	22.9 (10.7)	26.5 (13.0)	22.5 (13.1)	22.7 (11.6)
H-Y ("on")	2.60 (0.72)	2.68 (0.76)	2.49 (0.80)	2.60 (0.77)
H-Y ("off")	3.52 (0.80)	3.64 (0.80)	3.49 (0.90)	3.40 (0.77)
"Off" time, hours	7.13 (3.45)	6.76 (3.13)	6.51 (2.30)	7.62 (3.03)

Data are mean (SD) or number (%).

ZNS = zonisamide; PD = Parkinson disease; H-Y = Modified Hoehn and Yahr Scale score.

There were no significant differences between the ZNS and placebo groups with respect to changes from baseline in UPDRS Parts I, II, and IV scores and in the Modified Hoehn and Yahr Scale score.

Some patients showed increased duration of dyskinesia with increase of "on" time; however, the frequency of dyskinesia was not increased in the entire ZNS group compared with the placebo group. Further analysis showed a decrease in disabling dyskinesia (UPDRS Part IV, No. 33) in the 50-mg group (table 2). In addition, the basal dose of levodopa did not correlate with worsening or improvement of dyskinesia.

There was no significant difference in incidence of adverse events between the 25-mg (a total of 164 adverse events reported by 70.9% [56/79] of the patients) and 50-mg (195 adverse events reported by 72.9% [62/85] of the patients) groups, compared with the placebo group (153 adverse events by 65.1% [54/83] of the patients). However, the incidence of adverse events was significantly higher in the 100-mg group (204 adverse events reported by 79.5% [66/83] of the patients) compared with the placebo group ($p = 0.037$, χ^2 test). Adverse events with an incidence of greater than 5% in the ZNS group are presented in table 3. Adverse events for which the incidence was greater in the total ZNS than in the placebo group were somnolence (10.9%), apathy (8.5%), decrease in body weight (6.9%), and constipation (6.5%). Adverse events for which the incidence in the total ZNS was less than that of the placebo

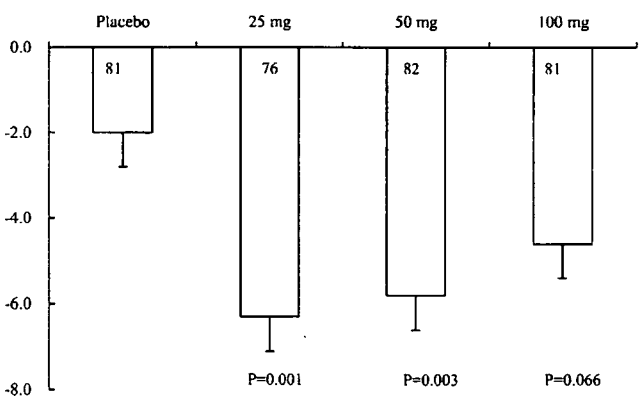

Figure 2. Changes in Unified Parkinson's Disease Rating Scale (UPDRS) Part III total score induced by zonisamide (ZNS) treatment from baseline to end of study (least-squares mean ± SE). Numbers indicate patient numbers. The total score of UPDRS Part III decreased after treatment in the 25-mg/day ($p = 0.001$) and 50-mg/day ($p = 0.003$) ZNS groups compared with the placebo group.

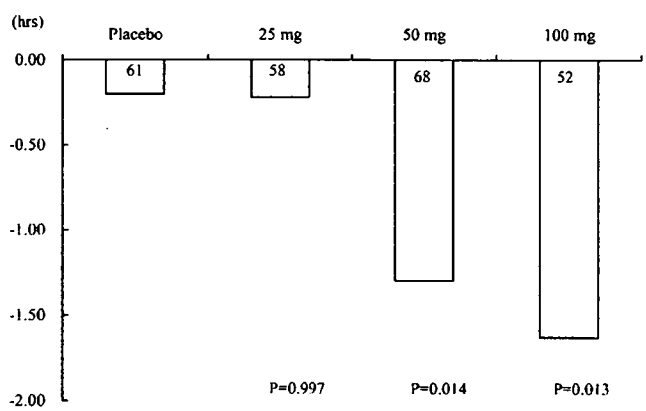

Figure 3. Changes from baseline in mean daily "off" time (hours) induced by treatment with zonisamide (ZNS). Numbers indicate patient numbers. "Off" time decreased after treatment with ZNS in the 50-mg/day (−1.3 hours, $p = 0.014$) and 100-mg/day (−1.63 hours, $p = 0.013$) groups compared with the placebo group.

Table 2 Changes in dyskinesia during 12-week treatment of zonisamide combined with anti-Parkinson disease drugs

	Placebo	ZNS		
		25 mg/day	50 mg/day	100 mg/day
Dyskinesia				
Baseline	28	18	33	22
Final assessment	28	21	29	22
Post-ZNS improvement	4	4	8	0
Post-ZNS worsening	1	2	5	4
Appearance during ZNS	1	5	0	1
Disabling dyskinesia				
Baseline	19	7	17	11
Final assessment	17	9	12	11
Post-ZNS improvement	5	1	7	3
Post-ZNS worsening	3	0	0	0
Appearance during ZNS	1	2	0	3

Data are number of patients. Dyskinesia (UPDRS Part IV, No. 32), Disabling dyskinesia (UPDRS Part IV, No. 33).

ZNS = zonisamide.

group were dizziness (5.7%), decrease in appetite (10.1%), and increase in serum creatinine phosphokinase (7.3%).

Discussion. In this study, ZNS adjunctive therapy significantly improved PD symptoms vs placebo, as indicated by the significant improvement in the UPDRS Part III total score for the primary endpoint in the 25-mg and 50-mg groups and significant mean decrease in total "off" time in the 50-mg and 100-mg treatment groups. The improvement in "wearing-off" was similar to the effects seen with rasagiline and entacapone, although neither drug improved the UPDRS Part III total score.[4] Although the randomized patients of our study used many anti-Parkinson concomitant medicines, they did not meet the requirements of adequate treatment of PD because of the attenuation of the beneficial effects. ZNS treatment improved all main PD symptoms in these patients, including tremor, similarly to previous reports.[2,3,5]

Interestingly, administration of ZNS did not increase the frequency of dyskinesia, and the frequency of both dyskinesia and disabling dyskinesia improved in the 50-mg group. The reason for the improvement in parkinsonian symptoms and disabling dyskinesia is not known at present. ZNS is not a glutamate antagonist, but it reduces glutamate release[6] and increases neuronal transporter excitatory amino acid carrier 1.[7] These actions of ZNS on the glutamate system may mediate the improvement of dyskinesia seen in our patients.

In this study, the mean basal levodopa dose was approximately 350 mg/day, although it is lower than that used in Western countries. In Japan, many physicians are using lower doses from therapeutic strategy and patients' preference for not having troublesome side effects. Cultural difference between Japan and Western countries may also affect the maintenance dose. Furthermore, the effective dopa plasma level in Western PD patients is 2,000 to

Table 3 Adverse effects associated with zonisamide treatment with an incidence of ≥5%

	Placebo	ZNS			
		All patients	25 mg/day	50 mg/day	100 mg/day
Somnolence	4.8	10.9	1.3	15.3	15.7
Apathy	6.0	8.5	7.6	7.1	10.8
Dizziness	7.2	5.7	3.8	5.9	7.2
Reduced appetite	14.5	10.1	5.1	8.2	16.9
Weight loss	4.8	6.9	7.6	3.5	9.6
Constipation	3.6	6.5	6.3	8.2	4.8
Increased in serum CK	8.4	7.3	8.9	8.2	4.8

Data are presented as percentage of incidence.

ZNS = zonisamide; CK = creatinine phosphokinase.

4,000 ng/mL[8] but that of Japanese patients is around 500 (max 1,000) ng/mL (unpublished data; data from 200 Japanese PD patients). Race, amount of protein intake, and physique may explain the difference in the effective levodopa dose between Western countries and Japan. The above data indicate that our patients were not undertreated with anti-PD drugs. In fact, our patients, like other Japanese patients with PD, developed treatment-related adverse effects during maintenance therapy using levodopa with or without other drugs. Nevertheless, further studies are necessary to evaluate ZNS in patients with PD treated with anti-PD drugs at doses commonly used in Western countries.

We started the study with a run-in period of single-blind treatment with placebo to minimize placebo effects. To the best of our knowledge, this is the most rigorous study design used to date for the evaluation of anti-Parkinson effects. Our study design may explain the lower response rate in the ZNS groups (although still significantly higher than placebo in the 25-mg and 50-mg study groups) than that of previous reports for pramipexole.[9]

Although there was a higher incidence of adverse events in the 100-mg group than in the other treatment groups, the incidence of hallucination and dyskinesia, which are typically of concern with anti-Parkinson drugs, was the same across all treatment groups, indicating that a once-daily dose of 25 to 100 mg of ZNS is well tolerated.

Although the present study was only of 12 weeks' duration, our preliminary data showed that the benefits observed at 12 weeks were maintained for more than 1 year in all 17 patients in a study on the long-term effects of ZNS on PD. Another study that was designed to assess the long-term (up to 1 year) effects of ZNS on PD (n = 100) also showed that 12-week course of ZNS improved parkinsonian symptoms and that such effects were maintained for up to 1 year (manuscript in preparation).

It is notable that the typical dose of ZNS is 300 to 600 mg/day for epilepsy, but a significant improvement in motor symptoms was noted in our patients with PD with only 50 mg/day of ZNS. This suggests that the mechanism of action of ZNS in PD may be different from those in epilepsy. In this regard, ZNS has multiple mechanisms of action. The major effect of ZNS in epilepsy is modification of neuronal firing at high frequency through enhancement of sodium channel inactivation and reduction of T-type calcium current.[10-13] ZNS has no affinity to γ-aminobutyric acid (GABA) type A receptor or glutamate receptors[11] but is known to increase GABA[6] and glutamate[7] release. In the dopaminergic system, therapeutic doses of ZNS (20 and 50 mg/kg) increase intracellular and extracellular dopamine levels in the rat striatum.[14-16] Conversely, supratherapeutic doses of ZNS reduce intracellular dopamine. Thus, ZNS has biphasic effects on the dopamine system. We reported previously that at therapeutic levels, ZNS increased dopamine synthesis by increasing tyrosine hydroxylase (TH) activity and TH messenger RNA.[14] ZNS also affects MAO-B activity. The IC_{50} (50% inhibitory concentration) value of MAO-B in liver microsomal fraction was 600 μM, and that in striatal membrane fraction was 28 μM.[14,17] These data suggest ZNS inhibits striatal MAO-B activity but not peripheral MAO-B activity, and therefore ZNS may have little effect on peripheral MAO-B inhibition of functions such as blood pressure.

Zonisamide has no affinity to dopamine receptors (D1–D5) or dopamine transporter. ZNS also has no direct effects on glutamate receptors, adenosine receptors, or serotonin receptors, which have been suggested as possible sites of action for anti-PD drugs, other than the dopaminergic system.[14] We proposed previously that activation of dopamine synthesis and moderate inhibition of MAO-B are the main mechanisms that mediate the effects of ZNS in PD.[14] However, the present finding of lack of change in the efficacy of ZNS when coadministered with an MAO-B inhibitor suggests that MAO-B inhibition is not a main factor. We consider that the primary mechanism of action of ZNS in PD is to increase dopamine synthesis. Whether sodium channel inactivation or T-type calcium channel inhibition is involved in ZNS effects has not been elucidated yet. Further investigation is needed to clarify the mechanism of the beneficial actions of ZNS on PD.

Appendix

The Japan Zonisamide on PD Study Group Investigators included the following members: H. Aizawa, MD, Asahikawa Medical College, Asahikawa; T. Kimura, MD, National Dohoku Hospital, Asahikawa; S. Kikuchi, MD, Hokkaido University, Sapporo; M. Baba, MD, Hirosaki University, Hirosaki; K. Chida, MD, National Iwate Hospital, Iwate; K. Hisanaga, MD, National Miyagi Hospital, Sendai; I. Toyoshima, MD, Akita University, Akita; K. Kurita, MD, Yamagata University, Yamagata; Y. Suzuki, MD, Nihonkai Hospital, Yamagata; K. Yoshizawa, MD, Mito Medical Center, Ibaraki; S. Shoji, MD, Tsukuba University, Ibaraki; I. Nakano, MD, Jichi Medical School, Tochigi; K. Hirata, MD, Dokkyo University School of Medicine, Tochigi; K. Kamakura, MD, National Defense Medical College, Saitama; T. Shimizu, MD, Teikyo University, Tokyo; S. Nogawa, MD, Keio University, Tokyo; H. Utsumi, MD, Tokyo Medical University, Tokyo; H. Mizusawa, MD, Tokyo Medical and Dental University, Tokyo; F. Yokochi, MD, Tokyo Metropolitan Fuchu Hospital, Tokyo; K. Hirabayashi, MD, Tokyo Metropolitan Ebara Hospital, Tokyo; K. Hasegawa, MD, National Sagamihara Hospital, Kanagawa; Y. Takahashi, MD, St. Marianna University, Kawasaki; Y. Kuroiwa, MD, Yokohama City University, Yokohama; S. Kameyama, MD, Nishi-Niigata Chuo National Hospital, Niigata; K. Komai, MD, Kanazawa University, Kanazawa; T. Hashimoto, MD, Shinsyu University, Matsumoto; K. Mizoguchi, MD, National Epilepsy Center Shizuoka, Shizuoka; S. Mitake, MD, Tosei General Hospital, Aichi; T. Yasuda, MD, Toyota Memorial Hospital, Aichi; Y. Washimi, MD, National Center for Geriatrics and Gerontology, Aichi; Y. Tatsuoka, MD, Tatsuoka Neurology Clinic, Kyoto; S. Matsumoto, MD, Kitano Hospital, Osaka; K. Abe, MD, Osaka University, Osaka; H. Fujimura, MD, Toneyama National Hospital, Osaka; H. Hashiguchi, MD, Nippon Steel Hirohata Hospital, Himeji; K. Nakashima, MD, Tottori University, Tottori; K. Takamatsu, MD, Brain Attack Center Oota Memorial Hospital, Hiroshima; T. Yamada, MD, Yamada Neurosurgery Hospital, Hiroshima; M. Nomoto, MD, Ehime University, Ehime; T. Yuhi, MD, University of Occupational and Environmental Health, Fukuoka; T. Yamada, MD, Fukuoka University, Fukuoka; K. Ikezoe, MD, Kyusyu University, Fukuoka; A. Sato, MD, Nagasaki Kita Hospital, Nagasaki; H. Matsuo, MD, National Hospital Organization Nagasaki Medical Center, Nagasaki; K. Tsuruta, MD, Koga General Hospital, Miyazaki; K. Arimura, MD, Kagoshima University, Kagoshima; T. Yuasa, National Center of Neurology and Psychiatry, Kohnodai Hospital, Ichikawa; N. Kawashima, MD, Kawashima Neurology Clinic, Kanagawa; A. Ishikawa, MD, Agano Hospital, Niigata; N. Yoshikawa, MD, Yoshikawa Clinic, Kobe; Y. Higashi, MD, Himeji Central Hospital, Himeji; H. Ohnishi, MD, Ohnishi Neurosurgical Center, Akashi; J. Yoshinaga, MD, City Hospital Hiroshima, Hiroshima; H. Fujita, MD, Murakami Memorial Hospital, Ehime; R. Katagi, MD, Katagi Neurological Surgery, Ehime; H. Miyajima, MD, Hamamatsu University School of Medicine, Hamamatsu; K. Ojika,

MD, Nagoya City University Hospital, Nagoya; and M. Kawamura, MD, Showa University Hospital, Tokyo.

References

1. Uno H, Kurokawa M, Masuda Y, Nishimura H. Studies on 3-substituted 1.2-benzisoxazole derivatives 6: syntheses of 3-(sulfamoylmethyl)-1,2- benzisoxazole derivatives and their anticonvulsant activities. J Med Chem 1979;22:180–183.
2. Murata M, Horiuchi E, Kanazawa I. Zonisamide has beneficial effects on Parkinson's disease patients. Neurosci Res 2001;41:397–399.
3. Murata M, Hasegawa K, Kanazawa I. Randomized, double-blind study of zonisamide with placebo in advanced Parkinson's disease. Mov Disord 2004;19: (suppl 9):S198.
4. Rascol O, Brooks D, Melamed E, et al. Rasagiline as an adjunct to levodopa in patients with Parkinson's disease and motor fluctuations (LARGO, Lasting effect in Adjunct therapy with Rasagiline Given Once daily, study): a randomized, double-blind, parallel-group trial. Lancet 2005;365:947–954.
5. Morita S, Miwa H, Kondo T. Effect of zonisamide on essential tremor: a pilot crossover study in comparison with arotinolol. Parkinsonism Relat Disord 2005;11:101–103.
6. Yoshida S, Okada M, Zhu G, Kaneko S. Effects of zonisamide on neurotransmitter exocytosis associated with ryanodine receptors. Epilepsy Res 2005;67:153–162.
7. Ueda Y, Doi T, Tokumaru J, Willmore LJ. Effect of zonisamide on molecular regulation of glutamate and GABA transporter proteins during epileptogenesis in rats with hippocampal seizures. Brain Res Mol Brain Res 2003;116:1–6.
8. Stocchi F, Vacca L, Ruggieri S, Olanow WC. Intermittent vs continuous levodopa administration in patients with advanced Parkinson disease. Arch Neurol 2005;62:905–910.
9. Mizuno Y, Yanagisawa N, Kuno S, et al. Randomized, double-blind study of pramipexole with placebo and bromocriptine in advanced Parkinson's disease. Mov Disord 2003;18:1149–1156.
10. Schauf CL. Zonisamide enhances slow sodium inactivation in Myxicola. Brain Res 1987;413:185–188.
11. Rock DM, Macdonald RL, Taylor CP. Blockade of sustained repetitive action potentials in cultured spinal cord neurons by zonisamide (AD 810, CI 912), a novel anticonvulsant. Epilepsy Res 1989;3:138–143.
12. Suzuki S, Kawakami K, Nishimura S, et al. Zonisamide blocks T-type calcium channel in cultured neurons of rat cerebral cortex. Epilepsy Res 1992;12:21–27.
13. Kito M, Maehara M, Watanabe K. Mechanisms of T-type calcium channel blockade by zonisamide. Seizure 1996;5:115–119.
14. Murata M. Novel therapeutic effects of the anti-convulsant, zonisamide, on Parkinson's disease. Curr Pharm Des 2004;10:687–693.
15. Okada M, Kaneko S, Hirano T, et al. Effects of zonisamide on dopaminergic system. Epilepsy Res 1995;22:193–205.
16. Gluck MR, Santana LA, Granson H, Yahr MD. Novel dopamine releasing response of an anti-convulsant agent with possible anti-Parkinson's activity. J Neural Transm 2004;111:713–724.
17. Okada M, Kaneko S, Hirano T, et al. Effects of zonisamide on extracellular levels of monoamine and its metabolites, and on Ca^{2+} dependent dopamine release. Epilepsy Res 1992;13:113–119.

Leucine-Rich Repeat kinase 2 G2385R variant is a risk factor for Parkinson disease in Asian population

Manabu Funayama[a], Yuanzhe Li[b], Hiroyuki Tomiyama[b], Hiroyo Yoshino[a], Yoko Imamichi[b], Mitsutoshi Yamamoto[c,f], Miho Murata[d,f], Tatsushi Toda[e,f], Yoshikuni Mizuno[a] and Nobutaka Hattori[a,b,f]

[a]Research Institute for Diseases of Old Age, [b]Department of Neurology, Juntendo University School of Medicine, Bunkyo-ku, Tokyo, [c]Department of Neurology, Kagawa Prefectural Central Hospital, Takamatsu, [d]Department of Neurology, Musashi Hospital, National Center of Neurology and Psychiatry, Tokyo, [e]Division of Clinical Genetics, Department of Medical Genetics, Osaka University Graduate School of Medicine, Suita, Osaka and [f]Core Research for Evolutional Science and Technology (CREST), Japan Science and Technology Agency, Saitama, Japan

Correspondence and requests for reprints to Dr/Professor Nobutaka Hattori, MD, PhD, Department of Neurology, Juntendo University School of Medicine, 2-1-1 Hongo, Bunkyo-ku, Tokyo 113-8421, Japan
Tel: +81 3 5802 1073; fax: +81 3 5800 0547; e-mail: nhattori@med.juntendo.ac.jp

Sponsorship: This study was supported by a grant from the Japan Foundation for Neuroscience and Mental Health (to M.F.).

Received 10 October 2006; accepted 23 October 2006

To assess the effect of genetic factors on sporadic Parkinson disease, we performed a case–control study of a variant (G2385R) in *Leucine-Rich Repeat kinase 2* among the Japanese population. The G2385R (c.7153G>A) variant was reported as a risk factor for sporadic Parkinson disease in the Chinese population from Taiwan and Singapore. Genotyping was conducted in 448 Parkinson disease patients and 457 healthy controls. The frequency of A allele in Parkinson disease was significantly higher than in the control ($P=1.24\times10^{-4}$, odds ratio 2.63, 95% confidence interval 1.56–4.35). Our results suggest that the G2385R variant is a risk factor for sporadic Parkinson disease in the Asian population. *NeuroReport* 18:273–275 © 2007 Lippincott Williams & Wilkins.

Keywords: *Leucine-Rich Repeat kinase 2*, risk factor, single nucleotide polymorphisms

Introduction

Parkinson disease (PD) is one of the most frequent neurodegenerative diseases characterized by resting tremor, rigidity, bradykinesia, and postural instability. PD is thought to be a multifactorial disease caused by a combination of aging, environmental, and genetic factors. Although the majority of patients of PD are of sporadic type, some genes have been identified as a monogenic causative gene by molecular genetic studies for familial PD [1–6]. *Leucine-Rich Repeat kinase 2* (*LRRK2*) has been identified as a causative gene associated with autosomal dominant familial PD [7,8]. To date, many pathogenic substitutions in *LRRK2* have been identified in familial and sporadic PD [9]. The G2385R variant (c.7153G>A) in *LRRK2* was reported recently as a risk factor for sporadic PD in the Chinese population from Taiwan and Singapore [10,11]. This variant was identified originally as putative pathogenic mutation in a small Taiwanese PD family and was not found in Caucasians [12]. Thus, it is possible that the G2385R variant is a risk factor in Asian sporadic PD. To test this hypothesis, we conducted a case–control study to evaluate the association between the G2385R genotype and the risk for PD in the Japanese population.

Methods

Subjects and genomic DNA

Genomic DNA was isolated from 448 sporadic PD patients and 457 controls of the Japanese population by a standard protocol (Table 1). All PD patients had no family history of PD. PD patients with *parkin* or *PTEN-induced putative kinase 1 (PINK1)* mutation were not included in the study. Diagnosis of PD was adopted by the participating neurologists and was established on the basis of the United Kingdom Parkinson's Disease Society Brain Bank criteria [13]. This study was approved by the ethics committee of Juntendo University School of Medicine. All individuals gave an informed and signed consent form.

Genotyping

Exon 48 of *LRRK2* from each individual was amplified by polymerase chain reaction (PCR) using the primers and protocol described by Zimprich *et al.* [8]. The PCR products were sequenced directly using the BigDye Terminators v1.1 Cycle Sequencing Kit (Applied Biosystems, Foster City, California, USA). The reverse PCR primer was used as sequencing primer.

Statistical analysis

Statistical analysis included the Hardy–Weinberg equilibrium test, χ^2 test, Fisher's exact test, odds ratio and its 95% confidence interval (95% CI), using SNPAlyze v5.1 software (Dynacom, Chiba, Japan). The *t*-test was performed using JMP 6.0 (SAS Institute Japan, Tokyo, Japan). In all statistical analyses, *P* values of 0.05 or less were considered statistically significant.

Results

We analyzed the frequency of the c.7153G>A (G2385R) substitution in 448 patients and 457 controls. Genotypes of the controls and patients were concordant with Hardy–Weinberg equilibrium. The frequency of A allele in the patients was significantly higher than in the controls ($P=1.24 \times 10^{-4}$, odds ratio 2.63, 95% CI 1.56–4.35, Table 2). We also detected homozygous substitution for the G2385R variant in two patients; however, we detected only the heterozygous substitution in the controls. Concerning the age at onset, the G2385R carriers were somewhat older than the noncarriers in total patients and in those <50 years of age. In contrast, the age at onset was not significantly different between carriers and noncarriers aged ≥50 years (Table 3). The disease duration was not significantly different between carriers and noncarriers (data not shown).

Discussion

In this study, we observed the *LRRK2* G2385R variant in 11.6% (52/448) of sporadic PD patients. So far, many putative pathogenic mutations have been reported including the G2385R. We detected G2385R in both patients and controls (22/457: 4.8%, Table 2); thus, this variant is not a pathogenic mutation, but a single nucleotide polymorphism. These results were similar to the allele frequencies in the Chinese [10,11]. It is estimated that mutations of *LRRK2* are the most frequent among the causative genes for autosomal dominant familial PD so far. Indeed, only one mutation (G2019S) accounted for ~6.6% of familial PD and ~1.6% of sporadic PD in Caucasians [14–16]. Interestingly, the frequency of the G2019S mutation is ~40% in the familial PD of North African Arabs [17] and ~30% in the familial PD of Ashkenazi Jews [18], whereas the G2019S mutation is a much less common mutation in Asians [19,20]. It is likely that some differences of genetic background exist among Caucasians, North African Arabs, Ashkenazi Jews, and Asians. Although G2385R has been detected only in Asian population, some risk variations in PD such as α-synuclein would be found in not only Asians but also all ethnic groups [21–24].

Among patients with age at onset <50 years, the G2385R carriers were somewhat older than noncarriers. This might indicate that G2385R has no influence on early-onset PD, and that PD of patients with early-onset might be influenced by other genetic and/or environmental factors. In addition, there were no differences in any clinical features including age at onset among carriers with homozygous or heterozygous G2385R substitution and noncarriers. Although the G2385R might increase the risk of development of PD, it does not seem to have a clear effect on modifying the symptoms or worsening the progression of the disease.

The amino-acid G2385 is located in the WD domain of LRRK2. This domain is known to bind various proteins [9]. The WD domain of LRRK2 appears to play an important role in neuronal cells. Indeed, oxidative-stress-induced cell death was more enhanced by the overexpression of G2385R variant than wild-type LRRK2 using culture cells [11]. More studies are needed to understand the functional significance of the substitution of glycine to arginine.

Conclusion

In this study, we identified that the G2385R variant in *LRRK2* is a risk for PD in Japanese population. To combine with the result of Chinese population [10,11], this variant increases the risk of PD in Asian population. So far, multiple genomic loci have been identified as susceptibility loci for PD [25], suggesting that many genes have a synergistic influence on the development of PD.

Table 1 Age characteristics of individuals

	Patients	Controls
Total sample, *n* (%)	448 (100)	457 (100)
Male, *n* (%)	217 (48.4)	240 (52.5)
Female, *n* (%)	231 (51.6)	217 (47.5)
Age at onset (years)[a]	50.7 ± 14.6 (5–89)	—
Male[a]	49.1 ± 14.8 (5–89)	—
Female[a]	52.2 ± 14.2 (7–82)	—
Age at sampling (years)[a]	59.4 ± 13.8 (15–93)	43.8 ± 16.0 (21–98)
Male[a]	57.8 ± 14.7 (15–93)	43.8 ± 14.5 (23–92)
Female[a]	60.9 ± 12.7 (22–88)	43.9 ± 17.5 (21–98)

[a]Data are mean ± SD (range).

Table 3 Comparison of age at onset of PD patients

Age at onset (years)	Carriers (*n*)	Noncarriers (*n*)	*P*-value
<50	42.5 ± 5.8 (17)	37.1 ± 9.4 (180)	0.003
≥50	59.9 ± 7.0 (33)	61.6 ± 7.8 (209)	0.24
Total	54.0 ± 10.6 (50)	50.3 ± 14.9 (389)	0.03

Data are mean ± SD.
Patients without information about age at onset (two of carriers and seven of noncarriers) were excluded from this analysis.
PD, Parkinson disease.

Table 2 Association analysis of *LRRK2* G2385R variant

	Genotype, *n* (%)			Allele, *n* (%)			
	G/G	G/A	A/A	G	A	χ^{2} [a]	*P*-value[a]
Patients (*n*=448)	396 (88.4)	50 (11.2)	2 (0.4)	842 (94.0)	54 (6.0)	14.74	1.24×10^{-4}
Controls (*n*=457)	435 (95.2)	22 (4.8)	0 (0)	892 (97.6)	22 (2.4)		

LRRK2, *Leucine-Rich Repeat kinase 2*.
[a]Compared with the control.

References

1. Polymeropoulos MH, Lavedan C, Leroy E, Ide SE, Dehejia A, Dutra A, *et al.* Mutation in the alpha-synuclein gene identified in families with Parkinson's disease. *Science* 1997; **276**:2045–2047.
2. Kitada T, Asakawa S, Hattori N, Matsumine H, Yamamura Y, Minoshima S, *et al.* Mutations in the parkin gene cause autosomal recessive juvenile parkinsonism. *Nature* 1998; **392**:605–608.
3. Leroy E, Boyer R, Auburger G, Leube B, Ulm G, Mezey E, *et al.* The ubiquitin pathway in Parkinson's disease. *Nature* 1998; **395**:451–452.
4. Bonifati V, Rizzu P, van Baren MJ, Schaap O, Breedveld GJ, Krieger E, *et al.* Mutations in the DJ-1 gene associated with autosomal recessive early-onset parkinsonism. *Science* 2003; **299**:256–259.
5. Singleton AB, Farrer M, Johnson J, Singleton A, Hague S, Kachergus J, *et al.* Alpha-synuclein locus triplication causes Parkinson's disease. *Science* 2003; **302**:841.
6. Valente EM, Abou-Sleiman PM, Caputo V, Muqit MM, Harvey K, Gispert S, *et al.* Hereditary early-onset Parkinson's disease caused by mutations in PINK1. *Science* 2004; **304**:1158–1160.
7. Paisan-Ruiz C, Jain S, Evans EW, Gilks WP, Simon J, van der Brug M, *et al.* Cloning of the gene containing mutations that cause PARK8-linked Parkinson's disease. *Neuron* 2004; **44**:595–600.
8. Zimprich A, Biskup S, Leitner P, Lichtner P, Farrer M, Lincoln S, *et al.* Mutations in LRRK2 cause autosomal-dominant parkinsonism with pleomorphic pathology. *Neuron* 2004; **44**:601–607.
9. Mata IF, Wedemeyer WJ, Farrer MJ, Taylor JP, Gallo KA. LRRK2 in Parkinson's disease: protein domains and functional insights. *Trends Neurosci* 2006; **29**:286–293.
10. Di Fonzo A, Wu-Chou YH, Lu CS, van Doeselaar M, Simons EJ, Rohe CF, *et al.* A common missense variant in the LRRK2 gene, Gly2385Arg, associated with Parkinson's disease risk in Taiwan. *Neurogenetics* 2006; **7**:133–138.
11. Tan EK, Zhao Y, Skipper L, Tan MG, Di Fonzo A, Sun L, *et al.* The LRRK2 Gly2385Arg variant is associated with Parkinson's disease: genetic and functional evidence. *Hum Genet* 2006; Sep 30 [Epub ahead of print].
12. Mata IF, Kachergus JM, Taylor JP, Lincoln S, Aasly J, Lynch T, *et al.* Lrrk2 pathogenic substitutions in Parkinson's disease. *Neurogenetics* 2005; **6**:171–177.
13. Hughes AJ, Daniel SE, Kilford L, Lees AJ. Accuracy of clinical diagnosis of idiopathic Parkinson's disease: a clinico-pathological study of 100 cases. *J Neurol Neurosurg Psychiatry* 1992; **55**:181–184.
14. Nichols WC, Pankratz N, Hernandez D, Paisan-Ruiz C, Jain S, Halter CA, *et al.* Genetic screening for a single common LRRK2 mutation in familial Parkinson's disease. *Lancet* 2005; **365**:410–412.
15. Gilks WP, Abou-Sleiman PM, Gandhi S, Jain S, Singleton A, Lees AJ, *et al.* A common LRRK2 mutation in idiopathic Parkinson's disease. *Lancet* 2005; **365**:415–416.
16. Di Fonzo A, Rohe CF, Ferreira J, Chien HF, Vacca L, Stocchi F, *et al.* A frequent LRRK2 gene mutation associated with autosomal dominant Parkinson's disease. *Lancet* 2005; **365**:412–415.
17. Lesage S, Durr A, Tazir M, Lohmann E, Leutenegger AL, Janin S, *et al.* LRRK2 G2019S as a cause of Parkinson's disease in North African Arabs. *N Engl J Med* 2006; **354**:422–423.
18. Ozelius LJ, Senthil G, Saunders-Pullman R, Ohmann E, Deligtisch A, Tagliati M, *et al.* LRRK2 G2019S as a cause of Parkinson's disease in Ashkenazi Jews. *N Engl J Med* 2006; **354**:424–425.
19. Tan EK, Shen H, Tan LC, Farrer M, Yew K, Chua E, *et al.* The G2019S LRRK2 mutation is uncommon in an Asian cohort of Parkinson's disease patients. *Neurosci Lett* 2005; **384**:327–329.
20. Tomiyama H, Li Y, Funayama M, Hasegawa K, Yoshino H, Kubo SI, *et al.* Clinicogenetic study of mutations in LRRK2 exon 41 in Parkinson's disease patients from 18 countries. *Mov Disord* 2006; **21**: 1102–1108.
21. Farrer M, Maraganore DM, Lockhart P, Singleton A, Lesnick TG, de Andrade M, *et al.* Alpha-synuclein gene haplotypes are associated with Parkinson's disease. *Hum Mol Genet* 2001; **10**: 1847–1851.
22. Pals P, Lincoln S, Manning J, Heckman M, Skipper L, Hulihan M, *et al.* Alpha-synuclein promoter confers susceptibility to Parkinson's disease. *Ann Neurol* 2004; **56**:591–595.
23. Mueller JC, Fuchs J, Hofer A, Zimprich A, Lichtner P, Illig T, *et al.* Multiple regions of alpha-synuclein are associated with Parkinson's disease. *Ann Neurol* 2005; **57**:535–541.
24. Mizuta I, Satake W, Nakabayashi Y, Ito C, Suzuki S, Momose Y, *et al.* Multiple candidate gene analysis identifies alpha-synuclein as a susceptibility gene for sporadic Parkinson's disease. *Hum Mol Genet* 2006; **15**:1151–1158.
25. Maraganore DM, de Andrade M, Lesnick TG, Strain KJ, Farrer MJ, Rocca WA, *et al.* High-resolution whole-genome association study of Parkinson disease. *Am J Hum Genet* 2005; **77**:685–693.

Neurobiology of Disease

The Induction Levels of Heat Shock Protein 70 Differentiate the Vulnerabilities to Mutant Huntingtin among Neuronal Subtypes

Kazuhiko Tagawa,[1] Shigeki Marubuchi,[1,2] Mei-Ling Qi,[1,3] Yasushi Enokido,[1] Takuya Tamura,[1] Reina Inagaki,[1] Miho Murata[3] Ichiro Kanazawa,[4] Erich E. Wanker,[5] and Hitoshi Okazawa[1,3,6]

[1]Department of Neuropathology, Medical Research Institute and 21st Century Center of Excellence Program for Brain Integration and Its Disorders, Tokyo Medical and Dental University, Tokyo 113-8510, Japan, [2]Toyama Chemical Company, Toyama 930-8508, Japan, [3]PRESTO, Japan Science and Technology Agency, Kawagoe 332-0012, Japan, [4]National Center for Neurology and Psychiatry, Kodaira 187-8502, Japan, and [5]Max-Delbrück Center for Molecular Medicine, D-13125 Berlin, Germany

The reason why vulnerabilities to mutant polyglutamine (polyQ) proteins are different among neuronal subtypes is mostly unknown. In this study, we compared the gene expression profiles of three types of primary neurons expressing huntingtin (htt) or ataxin-1. We found that heat shock protein 70 (*hsp70*), a well known chaperone molecule protecting neurons in the polyQ pathology, was dramatically upregulated only by mutant htt and selectively in the granule cells of the cerebellum. Granule cells, which are insensitive to degeneration in the human Huntington's disease (HD) pathology, lost their resistance by suppressing *hsp70* with siRNA, whereas cortical neurons, affected in human HD, gained resistance by overexpressing *hsp70*. This indicates that induction levels of *hsp70* are a critical factor for determining vulnerabilities to mutant htt among neuronal subtypes. CAT (chloramphenicol acetyltransferase) assays showed that CBF (CCAAT box binding factor, CCAAT/enhancer binding protein ζ) activated, but p53 repressed transcription of the *hsp70* gene in granule cells. Basal and mutant htt-induced expression levels of p53 were remarkably lower in granule cells than in cortical neurons, suggesting that different magnitudes of p53 are linked to distinct induction levels of *hsp70*. Surprisingly, however, heat shock factor 1 was not activated in granule cells by mutant htt. Collectively, different levels of *hsp70* among neuronal subtypes might be involved in selective neuronal death in the HD pathology.

Key words: **polyglutamine; transcriptome; hsp70; huntingtin; cell death; microarray**

Introduction

Susceptibilities to neurodegeneration are different among neuronal subtypes. Neuron subtype-specific cell death (selective neuronal death) remains one of the unsolved questions in the research of neurodegenerative disorders. One typical case of neuron subtype-specific cell death is amyotrophic lateral sclerosis in which lower and upper motor neurons are exclusively affected. Selective neuronal death is more or less observed in most human neurodegenerative diseases. For instance, striatal neurons and cortical neurons are severely affected in Huntington's disease, although granule cells in the cerebellum are preserved except in rare cases of homozygote or extremely long polyglutamine (polyQ) expansion. In spinocerebellar atrophies, however, striatal and cortical neurons are basically preserved. Because selective neuronal death is a critical feature of neurodegenerative disorders, elucidation of its underlying mechanisms is indispensable for our understanding of neurodegeneration.

Several hypotheses have been proposed to explain selective neuronal death. For instance, in the HD pathology, some researchers have proposed that aggregation-prone short peptides are selectively cleaved out of full-length proteins in striatal neurons (Li et al., 2000). In addition, regarding the HD pathology, phosphorylation of Ser421 is significantly reduced in the striatum *in vivo* (Warby et al., 2005). The phosphorylation of huntingtin at Ser421, which is mediated by Akt and stimulated by IGF-1 or FK506 (Humbert et al., 2002; Pardo et al., 2006), leads to reduction of the toxicity (Humbert et al., 2002; Colin et al., 2005; Warby et al., 2005). In the pathology of spinocerebellar ataxia type-1, several nuclear proteins such as LANP (leucine-rich acidic nuclear protein) and PQBP1 (polyglutamine tract binding protein 1) expressed in specific types of neuron have been implicated (Matilla et al., 1997; Okazawa et al., 2002). It is important to note that all the mechanisms proposed thus far provide explanations for the acceleration of neuronal dysfunction and/or cell death in specific neurons. The converse idea that a protective mechanism might function in specific neurons to make them resistant to the polyQ pathology, however, has not been tested.

An obvious approach to investigate the molecular mechanisms underlying the above-mentioned selective vulnerability would be to isolate the binding factors of the disease protein that are expressed in specific neuronal subtypes. This approach has

Received Aug. 13, 2006; revised Dec. 9, 2006; accepted Dec. 10, 2006.

This work was supported by grants from the Japan Science Technology Agency (PRESTO) and from the Ministry of Education, Culture, Sports, Science and Technology of Japan (16390249, 16650076, 18390254, 18650097; Research on Pathomechanisms of Brain Disorders, 17025017, 18023014) (H.O.). We thank Dr. Tomohiro Okuda (Toyama Chemical Company, Tokyo, Japan) for support in primary culture and Hiroko Ueda (Tokyo Metropolitan Institute for Neuroscience, Tokyo, Japan) for her excellent technical assistance. We also thank Dr. Richard Morimoto (Northwestern University, Evanston, IL) for providing the Hsp70-pr-Luciferase plasmid.

Correspondence should be addressed to Hitoshi Okazawa, Department of Neuropathology, Tokyo Medical and Dental University, 1-5-45, Yushima, Bunkyo-ku, Tokyo 113-8510, Japan. E-mail: okazawa-tky@umin.ac.jp.

DOI:10.1523/JNEUROSCI.4522-06.2007

 0270-6474/07/270868-13$15.00/0

actually succeeded in discovering several possible candidates (Matilla et al., 1997; Humbert and Saudou, 2002; Okazawa, 2003). Another approach would be to screen neuronal subtype-specific changes in transcriptome, proteasome, and metabolome. In this study, we performed a microarray analysis to analyze the difference in gene expression profiles of different neuronal subtypes under mutant polyQ protein expression.

We found that heat shock protein 70 (*hsp70*), a well known chaperone molecule that protects neurons against mutant polyQ proteins (Cummings et al., 1998, 2001; Warrick et al., 1999; Chai et al., 1999; Zhou et al., 2001; Adachi et al., 2003; Wacker et al., 2004), is selectively upregulated by mutant htt in granule cells resistant to HD. Furthermore, as a mechanism for the cell-specific regulation of *hsp70*, we found that p53 represses transcriptional upregulation of *hsp70* in vulnerable neurons like cortical neurons, but not in resistant neurons like cerebellar granule cells. This novel mechanism for neuron subtype-specific pathology may be useful for obtaining a better understanding selective neuronal death in neurodegeneration.

Materials and Methods

The preparation of RNA and cDNA. Total RNA was extracted from the cells and tissues with a Trizol reagent (Invitrogen, Carlsbad, CA). The synthesis of cDNA by reverse transcription was performed using an LA PCR kit version 2.1 (Takara, Tokyo, Japan) and an oligo-dT primer.

Microarray analysis. The total RNAs were labeled and hybridized with DNA microarrays according to the manufacturer's protocol. To start, the cDNAs synthesized from 10 μg of the total RNA were labeled with cyanine 3 (Cy3) or Cy5 using a fluorescence direct label kit (Agilent Technologies, Palo Alto, CA). Rat DNA microarrays, on which the cDNAs (mean length of 500 bases) of 14,811 genes were spotted, were hybridized with Cy3- and Cy5-labeled cDNAs at 65°C for 17 h. The gene chips were then washed with 0.5× SSC/0.01% SDS and 0.06× SSC at room temperature, dried, and scanned by a microarray scanner, CRBIOIIe (Hitachi, Tokyo, Japan). Data analyses were performed using DNASIS Array (Hitachi). After control spots and artifact signals were excluded, the signal intensity of a spot was calculated as the ratio of the total intensity of a given gene chip. Standardized signal intensities were scatter-plotted with Cy3 fluorescence on the *y*-axis and Cy5 fluorescence on the *x*-axis. We selected genes whose Cy3/Cy5 ratios were >3.0 or <0.33 for further analyses.

The primary culture of neurons. Primary neurons were prepared from the cerebral cortex or the striatum of 17-d-old Wistar rat embryos. Cerebellar neurons were prepared from Wistar rat pups at postnatal day 7 (SLC, Shizuoka, Japan). The rats were put under deep anesthesia with ether. Their brains were then dissected, minced into fine pieces, and rinsed with PBS. After incubation with 0.25% trypsin at 37°C for 20 min, the pieces were gently triturated with blue tips and filtered through a nylon mesh (Falcon 2350; Becton Dickinson, Bedford, MA) to remove any debris. Cells were then washed twice with culture medium containing 10% fetal bovine serum. For cortical and striatal neurons, DMEM (Nissui, Tokyo, Japan) containing 25 mM D-glucose, 4 mM L-glutamine, and 25 μg/ml gentamycin, was used. In addition, 25 mM KCl containing the above culture medium was used for the cerebellar granule neurons. Cells were seeded into dishes (Corning, Corning, NY) coated with poly-L-lysine (Sigma, St. Louis, MO) at 1.8×10^5 cells/cm^2, and cultured at 37°C and 5% CO_2. To remove proliferating glial cells, arabinosylcytosine (Sigma) was added to the culture medium (4 μM) on the following day.

HeLa cell culture. HeLa cells were maintained in DMEM (Sigma), which contained 10% fetal bovine serum (ICN Pharmaceuticals, Costa Mesa, CA), 100 U/ml penicillin (Invitrogen), and 100 μg/ml streptomycin (Invitrogen) in 5% CO_2 at 37°C.

Plasmid and cosmid construction. Rat cDNAs of *hsp70*, *Cbl-b*, *Omi*, *p53*, and CCAAT box binding factor (*CBF*) were isolated with reverse transcriptase PCR cloning. *Hsp70*, *Omi*, and *Cbl-b* cDNAs were amplified with the following primers: hsp70F (5′-CATGGCCAAGAAAACAGC-3′) and hsp70R (5′-CTAATCCACCTCCTCGATG-3′), OmiF (5′-GAGCCGAGGCGGAGCAG-3′) and OmiR (5′-TCAAACCCTTGCCAATCCAG-3′), or Cbl-bF (5′-CCGCTCGAGACGAAAGGACTAAGATTCCAG-3′) and Cbl-bR (5′-CCCAAGCTTCTATAGATTGAGACGTGGCG-3′) from cDNA of whole rat cerebellum, and subcloned into the *Stu*I site of pCR-Blunt (Invitrogen). The cDNAs of *hsp70* and *Omi* were then digested with *Eco*RI from the Hsp70/pCR-Blunt and Omi/pCR-Blunt. cDNA of *Cbl-b* was cloned into the *Xho*I and *Hind*III sites of pBluescript I SK+ (Toyobo, Osaka, Japan). The inserts were subsequently cleaved out with *Eco*RI or *Xho*I-*Hind*III, respectively. They were then subcloned in the *Swa*I site of the pAxCAwt cosmid (Takara) after blunting of the inserts with a Blunting High kit (Toyobo). The *p53* gene was amplified with primers p53F (5′-GGAATTCCATGGAGGATTCACAGTCGG-3′) and p53R (5′- ACGCGTCGACTCAGTCTGAGTCAGGCCCC-3′) from the cDNA of rat cerebellum primary neurons. They were subcloned into the *Eco*RI and *Sal*I sites of pBluescript II SK+ and then digested with *Eco*RI-*Sal*I and recloned into the *Eco*RI and *Sal*I sites of pCIneo. The *CBF* gene likewise was amplified with primers CBFF (5′-ACGCGTCGACAATGTCGGCGGACCAGGAA-3′) and CBFR (5′-ATAAGAATGCGGCCGCTCACTTCCTTTGTCTTTTGGG-3′) from the cDNA of rat cerebellum primary neurons, and then cloned into the *Sal*I and *Not*I sites of pBluescript II SK+. To construct expression vectors of *Cbl-b* with a FLAG sequence at the N terminus, blunted *Nhe*I and *Not*I fragments of CBF were subcloned into the *Sal*I and *Not*I sites of pCIFm, which contained a FLAG sequence at the *Not*I site of pCIneo (Stratagene, La Jolla, CA). The plasmids were designated pCI-FLAG-Cbl2 and pCI-FLAG-CBF, respectively.

Adenovirus. The cosmid of rat hsp70-, Cbl-b-, and Omi-pAxCA, were transfected into 293 cells through the calcium-phosphate method using the digested DNA of adenoviruses. After the cells expired, the medium was recovered as the virus solution. We then rechecked the construction of the adenovirus vectors through PCR and confirmed that the E1A protein was deleted and that the insert was maintained correctly. After the check, we amplified the adenoviruses two to three times. We designated the adenovirus vectors as AxCA-Hsp70, AxCA-Cbl-b, and AxCA-Omi. The vectors were used to infect HeLa cells and primary neurons at a multiplicity of infection of 300 and 100, respectively. Adenovirus, AxCA-htt(exon1)20Q, -htt(exon1)111Q, -Atx30Q, and -Atx82Q, were constructed as described previously (Hoshino et al., 2003, 2004; Tagawa et al., 2004). The adenovirus vectors contain the htt exon-1 peptide or the full-length ataxin-1 (Atx-1) protein.

Western blotting analysis of cells and human brains. For Western blot sampling, whole cells were dissolved in 62.5 mM Tris/HCl, pH 6.8, 2% (w/v) SDS, 2.5% (v/v) 2-mercaptoethanol, 5% (v/v) glycerin, and 0.0025% (w/v) bromophenol blue on culture dishes. The cell lysates were collected from six-well dishes containing 3.3×10^4 cells/well (HeLa and 293 cells) and wells containing 1.0×10^5 primary neurons/well. Human brain samples were prepared from six Huntington's disease patients confirmed by CAG repeat expansion (grade 1–5; 43- to 60-year-old) and from six nonfamilial Parkinson's disease (PD) patients (Yahr's stage 1–5; 46- to 73-year-old). Brains of the age-matched non-neurological disease patients were used as the control. In these cases, 1-mm-thick tissues were carefully prepared under the microscope from the brain surface of the prefrontal cortex or cerebellar hemisphere cortex of these patients and used for the analysis. Brain samples of mutant htt-transgenic R6/2 mice (Mangiarini et al., 1996), B6CBA-Tg(HDexon1)62Gpb/1J (The Jackson Laboratory, Bar Harbor, ME), were prepared similarly at the age of 4 or 14 weeks. These samples were separated by SDS-PAGE, transferred onto polyvinilydene difluoride membrane Fine Traps (Nihon Eido, Tokyo, Japan) through a semidry method, blocked by 5% milk in TBS with Tween 20 (TBST) (10 mM Tris/Cl, pH 8.0, 150 mM NaCl, 0.05% Tween 20), and incubated with appropriate antibodies as described previously (Tagawa et al., 2005). The filters were incubated with each primary antibody for 2 h, with the corresponding horseradish peroxidase (HRP)-conjugated second antibody at a 1:3000 dilution for 1 h at room temperature in 5% milk/TBST. Finally, the target molecules were visualized through an enhanced chemiluminescence Western blotting detection system (Amersham Biosciences, GE Health Care Biosciences, Hong Kong).

Immunocytochemistry. The cells were fixed in 1% paraformaldehyde/0.1 M PBS, pH 7.4, for 30 min, and permeabilized with 0.1% Triton X-100 in PBS for 5 min at room temperature. Subsequently, the cells were

washed with PBS, blocked with 0.5% milk in PBS for 30 min at room temperature, and incubated with primary antibodies in PBS containing 0.5% milk for 2 h at room temperature. Anti-polyQ antibody CAG53b was diluted at a ratio of 1:10,000 and anti-hsp70 antibody (K20, Santa Cruz Biotechnology, Santa Cruz, CA) was diluted to 1:100. Incubation with the secondary antibodies, Alexa Fluor 350, 488, and 588- labeled anti-IgGs (Invitrogen), diluted at 1:1000 in 0.5% milk in PBS, was performed for 30 min at room temperature. We calculated their signal intensities per area as described previously (Hoshino et al., 2003).

The immunohistochemistry of human brain tissues. Postmortem brain tissues were prepared from three HD patients confirmed by CAG repeat expansion and one from disease control. The paraffin-embedded sections were deparaffinized, rehydrated, and then autoclaved in 10 mM of citrate buffer, pH 6.0, at 120°C for 15 min. These sections were incubated sequentially with 3% hydrogen peroxide for 20 min at room temperature to inhibit endogenous peroxidase, then with 1.5% normal goat serum in PBS for 30 min at room temperature, followed by incubation with primary antibodies against hsp70 (K20) for overnight at 4°C, and finally with Envision+ anti-rabbit or -mouse (Dako, High Wycombe, UK) for 3 h at room temperature. The anti-hsp70 antibody was used at a 1:200 dilution, washed with 0.1% Tween 20–TBS (TNT) buffer twice, and incubated with an HRP-conjugated secondary antibody (1:3000; GE Healthcare) for 1 h at room temperature (RT). The antibodies were then washed again with TNT buffer twice, and visualized through incubation with FITC tyramide (1:200; Perkin-Elmer, Boston, MA) for 10 min. The tyramide complex was stripped through incubation with 0.05 M glycine-HCl at pH 3.6 for 3 h at RT.

RNA interference. The cells were transfected with siRNA oligonucleotides using Lipofectamine 2000 (Invitrogen) according to the manufacturer's instructions. A total of 2.5×10^4 cells in six-well dishes were infected with 0.5 μg siRNA/well, 24 h after plating. The siRNAs corresponding to *hsp70* mRNA were designed with two base overhangs (dTdT) on each strand, and chemically synthesized by Qiagen (Hilden, Germany). The targeted sequences were Hsp70-siRNA#1 (5′-AAGGTGCAGGTGAACTACAAG-3′) and Hsp70-siRNA#2 (5′-AACACGCTGGCTGAGAAAGAG-3′). A verified siRNA against CBF was purchased from Qiagen (Mm Cebpz 1 HP siRNA, SI00948451).

Cell death assays (trypan blue staining). The cells were incubated for 5 min in a solution of 0.4% trypan blue (Invitrogen). In each experiment, blue stained (nonviable) and nonstained (viable) cells were counted in 10–20 visual fields, randomly selected at 100× magnification from each of three dishes. We counted at least 1000 cells for each condition.

Cell fractionation. The cells were harvested by scraping, collected in PBS, and then centrifuged for 4 min at 480 g and 4 C. The pellet was suspended in eight volumes of lysis buffer (20 mM HEPES, pH 7.9, 1 mM EDTA, pH 8.0, 1 mM dithiothreitol, 10% glycerol, 0.5 mM spermidine, 1 mM phenylmethylsulfonyl fluoride, 1 μg/ml pepstatin A, 0.3 μg/ml antipain, and 1 μg/ml leupeptin), to which NP-40 was added, making a final concentration of 0.3%, then homogenized by 10 strokes of a Dounce homogenizer type B. The separated nuclei in the homogenate were checked microscopically. The homogenate was centrifuged at 11,100 g at 4°C, for 10 min. The pellet and supernatant were nuclear and cytosolic fractions, respectively.

CAT (chrolamphenicol acetyltransferase) assay. To construct reporter plasmids, the human *hsp70* promoter region (198bp), was amplified by using the following primers: hHsp70proF (5′-CCGCTCGAGGAAG AGTCTGGAGAGTTCTG-3′) and hHsp70proR (5′-CCCAAGCTT-CCGGA CCCGTTGCCCCT-3′) from human genomic DNA (G1471, male; Promega, Madison, WI), and subcloned into the *Xho*I and *Hind*III sites of p0CAT. The resultant plasmid was designated as hHsp70pro. The deletion plasmids of the proximal or distal CCAAT elements were constructed by PCR with the following primers: Hsp70pro-dproCCAAT-F (5′-CTCAGAAGGGAAAAGGCGG-3′) and Hsp70pro-dproCCAAT-R (5′-ACCGAGCTCGATGAGGCTG-3′), or Hsp70pro-ddisCCAAT-F (5′-TCCAAGGAAGGCTGGGGG-3′) and Hsp70pro-ddisCCAAT-R (5′-AGAGGCCAGAGTGCCGCC-3′), from Hsp70pro/p0CAT. The deletion plasmid of both CCAAT elements was constructed with the primers, hHsp70proF and hHsp70proR, from hHsp70pro-ddisCCAAT/p0CAT. Ten micrograms of reporter and effector plasmids were transfected into 1×10^6 HeLa cells and neurons using a Superfect reagent (Qiagen) or a Lipofectamine Plus reagent (Invitrogen) according to commercial protocol. Forty-eight hours after transfection, cells were harvested with 0.25 M Tris-HCl, pH 7.5, and CAT assays were performed as described previously (Okamoto et al., 1990; Okazawa et al., 1991).

ChIP assay. A ChIP assay was performed according to the method described previously (Shang et al., 2000), with only minor modifications. Because no antibody was available for detecting CBF, the primary cerebellar neurons were transfected using the pCI-FLAG-CBF with Lipofectamine 2000 (Invitrogen). After 2 d, formaldehyde was added directly to the culture medium of the primary neurons for a final concentration of 1% to cross-link DNA and nuclear proteins. The medium was then incubated for 10 min at room temperature. After terminating the cross-linking with glycine, the cells were washed extensively and harvested in the presence of protease inhibitors. Nuclei were then separated and chromatin was sonicated to ~600 bp fragments. After a preclearance with a salmon sperm DNA/protein agarose slurry, anti-FLAG M2 monoclonal antibody (Sigma) was used at a 1:500 dilution and incubated overnight at 4°C for immunoprecipitation of the DNA-protein complex. Anti-p53 antibody (R-19; Santa Cruz Biotechnology) was similarly used at a 1:1000 dilution. After standard washing and elusion procedures, cross-linking was reversed by incubation with RNase in 0.3 M NaCl for 5 h at 65°C. The DNA was then precipitated using a 0.5 vol of ethanol treated with 4 mg/ml proteinase K, purified with QiaQuick spin columns (Qiagen), and used as a template for PCR. The primers 5′-TACCTCATCATGTT-TGGTGC-3′ and 5′-CGTTTGGCTTGCTAGGCAAG-3′ were used to amplify 280 bp surrounding the CCAAT box at −287 of the rat *hsp70* gene.

Results

Integrative analyses of gene expression profiles suggest multiple candidate genes

To explore the molecular mechanisms underlying the selective pathology of polyQ diseases (i.e., distinct susceptibilities of different neurons to different polyQ proteins), we performed DNA microarray analyses with three types of primary neurons (cortical, striatal, and cerebellar neurons) expressing either htt or Atx-1, and compared the expression profiles of 14,000 genes among them. Our reasons for using primary neurons instead of human or mouse brain tissues are as follows: (1) to exclude the contamination of glial or vascular cells from the analysis, (2) to detect early changes in gene expression (i.e., expression profiles at the starting point of aggregate formation), and (3) to compare easily multiple combinations of disease genes and neuron subtypes. Before starting the microarray analysis, we checked the expression levels of two polyQ genes in three types of neurons (supplemental Figs. 1, 2, available at www.jneurosci.org as supplemental material) and confirmed the expression levels of a polyQ protein to be almost equivalent in three subtypes of neurons and the expression levels of different polyQ proteins to be almost equivalent in a subtype of neurons.

To delineate changes in gene expression that might be relevant to the selective neuronal death or dysfunction, we compared the gene expression profiles of multiple neuronal subtypes under mutant and normal polyQ protein expression by adenovirus vectors at 2 d after infection, when only a very few neurons show inclusion bodies (Tagawa et al., 2004). The expression efficiencies of htt and Atx-1 proteins by adenovirus vectors in primary neurons have been examined previously (Tagawa et al., 2004; Hoshino et al., 2003, 2004). As described in those methods, the E1A protein was deleted in our adenovirus vectors to prevent viral proliferation. The viruses can proliferate in only 293 cells stably expressing the E1A protein. The expression of mutant htt by the adenovirus vector induces cell death in a small percentage of neurons by 4 d of infection (Tagawa et al., 2004). Therefore, RNA samples prepared on day 2, when cell death is not yet detectable (Tagawa et al., 2004), were used in microarray analyses,

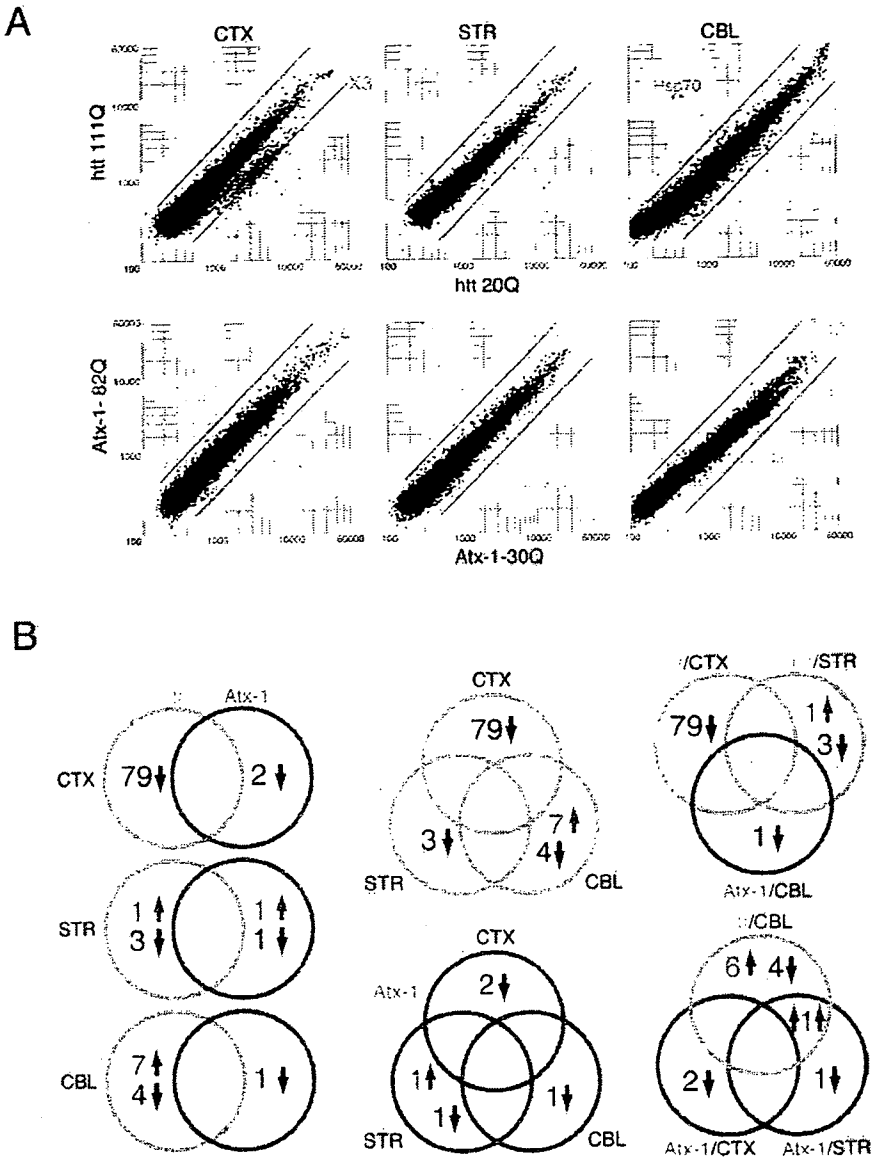

Figure 1. The microarray analyses with three neuron subtypes expressing Atx-1 or htt. *A*, Cortical neurons (CTX), striatal neurons (STR), and cerebellar neurons (CBL). The vertical bar of the graph indicates the signal intensities of the spots on the microarray in mutant polyQ gene expression, and the horizontal bar indicates the signals in normal polyQ gene expression. Green bars indicate thresholds of threefold. For the generation of probes, primary neurons were infected with adenovirus vectors of normal or mutant polyQ disease genes (*htt* or *Atx-1*) and mRNA was prepared at 2 d after infection. *B*, A comparison of genes whose expression was changed more than threefold. Left panels show a comparison between *Atx-1* and *htt* in each neuron subtype. Middle panels are analyzed with different types of polyQ genes. The top right panel includes vulnerable combinations, and the bottom right panel indicates resistant combinations.

to prevent the detection of secondary changes by cell death. Using this protocol, we infected three types of primary neurons with the adenovirus vectors of the full-length protein of Atx-1 or the htt exon-1 peptide (Tagawa et al., 2004) and prepared mRNA.

Six sets of analyses were conducted using two polyQ disease genes and three types of primary neurons (Fig. 1*A*). In each set, we compared the gene expression profiles under mutant polyQ and normal polyQ expression two times. We then selected genes whose expression was changed more than threefold (Fig. 1, supplemental Tables 1, 2, available at www.jneurosci.org as supplemental material). Next, we compared the changed genes among different sets in terms of neuron-type, disease gene, and susceptibility of neurons, to select candidate genes that might be relevant to the pathology (Fig. 1*B*).

The first notable observation from the comparison was that there was no overlap among the groups except in the case of one gene upregulated by the expression of mutant htt in cerebellar neurons, and by Atx-1 in striatal neurons (Fig. 1*B*, bottom right). This gene, heterogeneous nuclear ribonucleoprotein H (hnRNPH), has been identified as a component of htt aggregates previously (Hazeki et al., 2002), although its implication in the pathology has not been clarified in detail.

From the comparison, we selected the following candidate genes that were changed selectively in the vulnerable neurons or in the resistant neurons. *Omi/HtrA2* and *Cbl-b/Cbl-2* were downregulated by mutant htt selectively in the striatal neurons that are most vulnerable to HD. *Hsp70*, however, was upregulated by mutant htt in cerebellar neurons not affected by HD. Although some of these genes may be involved in the disease's pathology (R. Inagaki, M.-L. Qi, and H. Okazawa, unpublished observation), we focus only on *hsp70* in this paper.

Mutant htt but not mutant Atx-1 induces the upregulation of *hsp70* specifically in cerebellar neurons

hsp70 was outstanding regarding the extent of change of gene expression. In primary cerebellar neurons (most of them are granule cells) expressing mutant htt, *hsp70* was upregulated to a magnitude of ~30-fold. Interestingly, the change was considered specific because *hsp70* was not altered in primary striatal or cortical neurons, and because Atx-1 did not affect *hsp70* in cerebellar neurons (Fig. 1, supplemental Tables 1, 2, available at www.jneurosci.org as supplemental material). In addition, adenovirus vectors expressing polyQ genes lacked the E1A protein. The upregulation of *hsp70* was not observed in adenovirus-infected neurons other than htt-expressing cerebellar neurons (Fig. 1*A*). Therefore, although the E1A virus protein could induce *hsp70* (Kao et al., 1985; Wu et al., 1986; Williams et al., 1989), *hsp70* was not upregulated by E1A, but instead by the mutant htt in our experiments with E1A-deficient adenovirus vectors. These results collectively suggest that *hsp70* is another candidate gene that regulates neuron type-specific cell death.

The first question we asked in the present study was, whether the upregulation of *hsp70* gene expression led to an increase in the hsp70 protein. Western blot analyses of primary neurons clearly showed a remarkable increase in the hsp70 protein at a magnitude of 8 folds, and the change was observed specifically in the cerebellar neurons expressing mutant htt (Fig. 2*A*,*B*). Although a similar response was not found in most non-neuronal cell lines, we found that HeLa cells did show a similar increase of hsp70 by mutant htt (Fig. 2*C*). Therefore, we conducted a second experi-

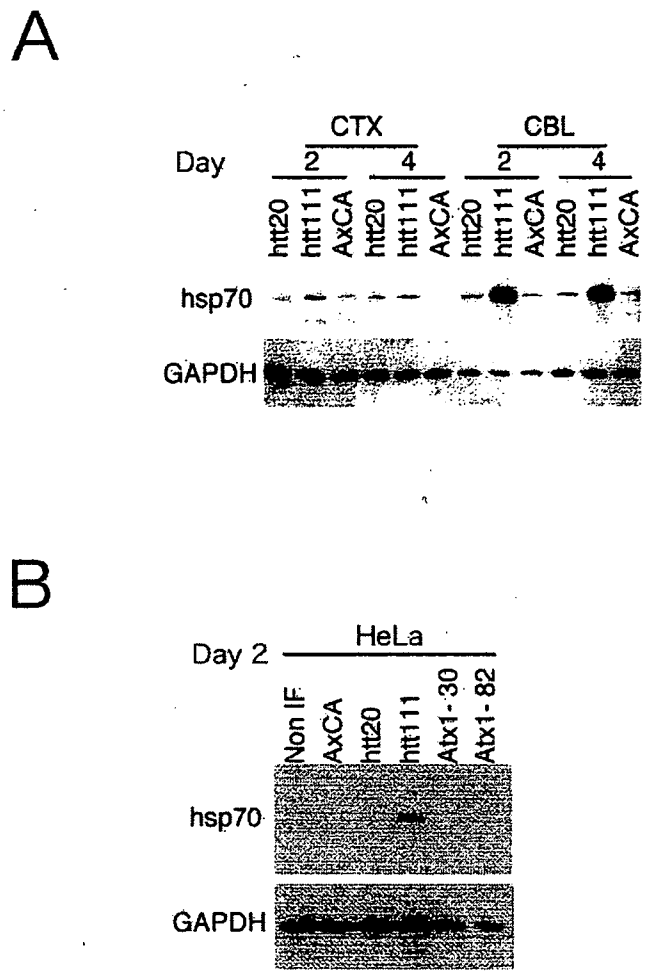

Figure 2. Hsp70 protein is induced by mutant htt specifically in cerebellar neurons. *A*, Western blot analyses showed that the expression of htt(exon1)111Q remarkably increased the hsp70 protein in cerebellar neurons (CBL), whereas htt(exon1)20Q or empty virus vectors did not affect hsp70. Mutant htt did not affect expression of hsp70 in cortical neurons (CTX) or in striatal neurons (data not shown). Days indicate the duration between adenovirus infection and sampling. *B*, HeLa cells show the remarkable response of hsp70 to mutant htt similar to that in cerebellar neurons. Normal and mutant Atx-1 (Atx1–30 and Atx1–82) did not affect hsp70 in HeLa cells.

ment using HeLa cells in parallel with primary neurons to analyze molecular mechanisms relevant to *hsp70* upregulation.

Despite the dramatic increases in *hsp70*, other heat shock proteins such as *hsp40*, *hsp84*, *hsp105α*, and *MRJ*, did not change remarkably in our microarray and Western blot analyses (data not shown). Microarray analysis did not detect a change in *hsc70* (cellular cognate form) in any of the six combinations of neurons and polyQ genes (data not shown). Although *hsp27* increased remarkably in microarray analyses, the protein increase was not confirmed by Western blots (data not shown). Therefore, upregulation of *hsp70* by the mutant htt represents a highly specific change in cerebellar neurons.

Next, we examined the relationship between the mutant htt aggregation and *hsp70* upregulation (Fig. 3*A*). The CAG53b antibody, which reacts with hard aggregates more strongly than preaggregates of mutant polyQ (Tagawa et al., 2004), revealed that hsp70 increases in primary cerebellar neurons possessing inclusion bodies of mutant htt (Fig. 3*A*). As has been reported previously in other studies (Jana et al., 2000; Krobitsch and Lindquist, 2000; Muchowski et al., 2000; Wyttenbach et al., 2000; Waelter et al., 2001a; Wyttenbach et al., 2001; Zhou et al., 2001), the hsp70 protein is partially colocalized with the mutant htt in inclusion bodies (Fig. 3*A*). To confirm that mutant htt and mutant Atx-1 were expressed at equivalent levels in cerebellar neurons, we further performed immunocytochemistry with CAG53b and 1C2 antibodies (Fig. 3*B*). Although these antibodies detected different distributions and different aggregation states of the mutant proteins, total expression levels were collectively almost equivalent between mutant htt and Atx-1 (Fig. 3*B*).

We also examined whether hsp70 increases in the granule cells of human patient brains by immunohistochemical analyses (Fig. 4). We found that the signal intensities of hsp70 in the granular layer were significantly increased in HD patients in comparison to the control (Fig. 4*A–D*). However, the signals were not changed in the molecular layer and in Purkinje cells (Fig. 4*E,F*). In the cerebrum, the cortical neurons possessed similar levels of hsp70 in both the patients and the controls (Fig. 4*G,H*).

Furthermore, we performed Western blotting with human brain tissue specimens. We detected an obvious increase of hsp70 protein in the cerebellar cortex of the mild HD cases (grade 1–3) in comparison to the Parkinson's disease brains, but not in the frontal lobe cortex of the cerebrum (Fig. 5*A*). Interestingly, the change was diminished in advanced HD patients (grade 4 or 5). To rule out postmortem changes of hsp70 protein, we performed similar experiments with the R6/2 mutant htt-transgenic mice. In this case, we detected an upregulation of hsp70 both in the presymptomatic mice at 4 weeks and in the symptomatic mice at 14 weeks (Fig. 5*B*). These results support the significance of the upregulation of *hsp70* in the human HD pathology.

Hsp70 expression levels regulate susceptibility of primary neurons to mutant htt

Hsp70 attenuates neurotoxicity in different model systems of polyQ diseases *in vivo* (Cummings et al., 1998, 2001; Chai et al., 1999; Warrick et al., 1999; Zhou et al., 2001; Adachi et al., 2003; Wacker et al., 2004). To address whether upregulation of *hsp70* also diminishes htt(exon1)111Q-induced neurotoxicity in cerebellar neurons, RNAi experiments were performed to selectively downregulate hsp70. We found that the siRNA/Hsp70#1 downregulated the hsp70 protein level to 50% in cerebellar neurons (Fig. 6*A*, left). When the cell death was quantified by a trypan blue assay, the decrease of hsp70 enhanced the toxicity of mutant htt in cerebellar granule cells (Fig. 6*A*, right). In contrast, the siRNA/Hsp70#2, which did not reduce hsp70 levels, had no effect on cell death by mutant htt (Fig. 6*A*). Simultaneously to this exploration, we examined whether hsp70 expression increases the resistance of cortical neurons to mutant htt. As expected, cortical neurons that overexpress hsp70 became resistant to mutant htt (Fig. 6*B*). These results collectively suggest that the expression levels of *hsp70* critically regulate the susceptibility of primary neurons to mutant htt.

To test whether the *hsp70* induction affects the formation of inclusion bodies, we stained the htt(exon1)111Q-expressing neurons after a siRNA/Hsp70#1 treatment with N-18 and 1C2 antibodies. The RNAi treatment decreased the percentage of N-18 stained inclusion-positive cells from 13.9 to 10.5%, whereas the signals from 1C2 staining became stronger by suppression of *hsp70* (data not shown).

Hsp70 upregulation in granule cells is not mediated by HSF1

To investigate the transcriptional regulation of *hsp70* in response to mutant htt, we firstly inquired into the involvement of heat shock factor 1 (HSF1), a well known transcription factor regulat-

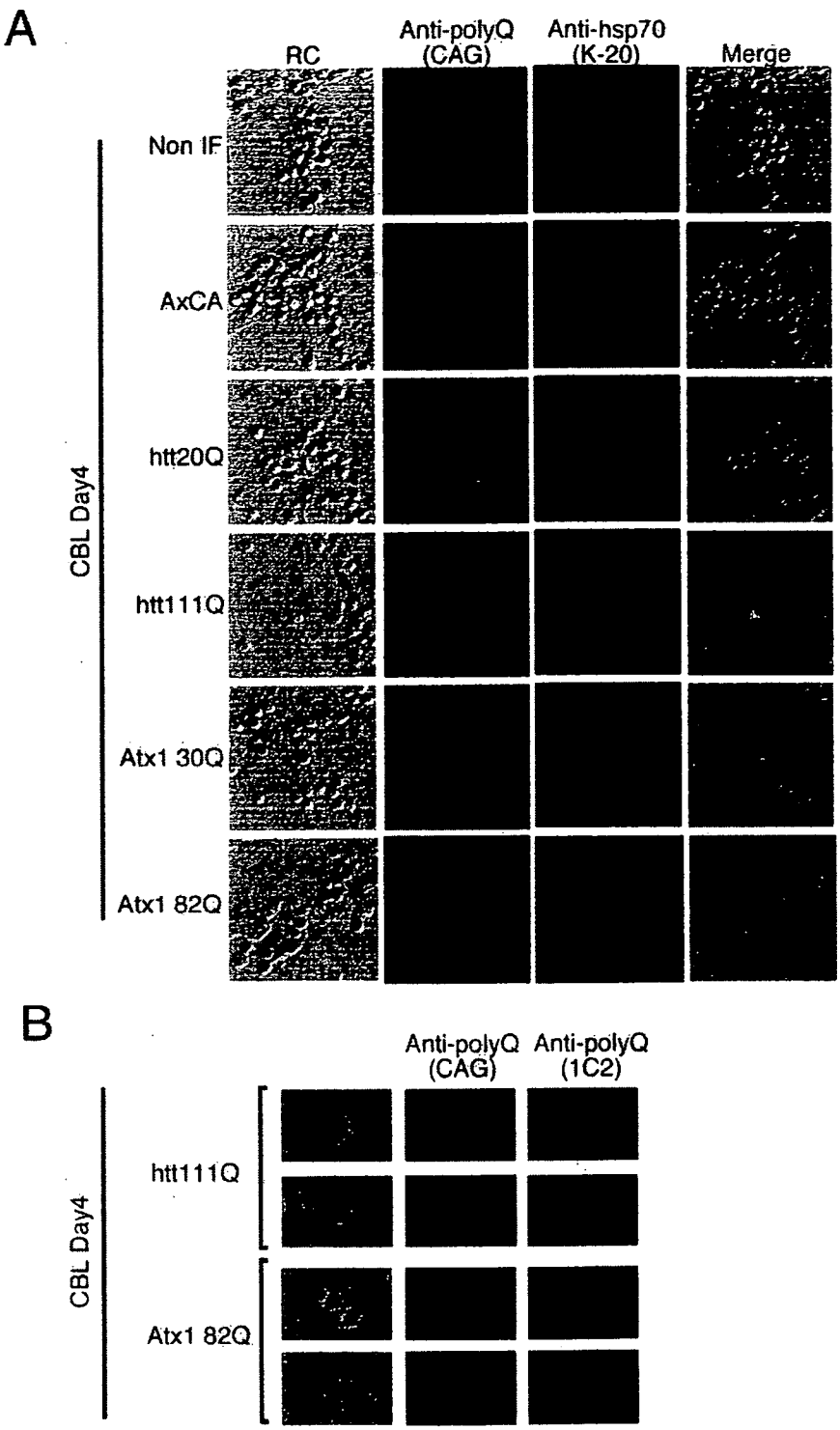

Figure 3. The induction levels of hsp70 correlate with expression levels of mutant htt in cerebellar neurons. Normal and mutant polyQ disease proteins were expressed in cerebellar neurons by adenovirus vectors. Four days after infection, neurons were stained with the CAG53b antibody (Scherzinger et al., 1997) that detects both Atx-1 and htt (Tagawa et al., 2004). Neurons expressing mutant htt at high levels showed a remarkable increase of hsp70. The expression levels of htt and Atx-1 are shown in supplemental Figures 1 and 2 (available at www.jneurosci.org as supplemental material).

ing heat shock proteins. HSF1 plays a central role in the transcriptional regulation of multiple heat shock proteins (Pirkkala et al., 2001). In response to various stimuli such as heat, oxidants, and heavy metals, the phosphorylation and translocation of HSF1 into the nucleus are induced (Pirkkala et al., 2001). Phosphorylated HSF1 binds to heat-shock elements locating upstream to heat shock protein genes, and upregulates transcription from those genes. There is no doubt that HSF1 generally activates transcription from the *hsp70* gene. However it does not mean that endogenous HSF1 is actually activated in the HD pathology.

Therefore, in this study, we examined whether mutant htt expression activates HSF1 in granule cells. Unexpectedly, immunocytochemistry revealed that mutant htt expression does not induce translocation of HSF1 to the nucleus (Fig. 7*A*), although it is indispensable for the activation of HSF1. Consistently, the Western blotting findings did not show a shift of HSF1 from the cytoplasmic fraction to the nuclear fraction (supplemental Fig. 3, available at www.jneurosci.org as supplemental material). Furthermore, the phosphorylation of Ser230 of HSF1, which has a positive effect on the transactivating capacity of HSF1, was not induced by mutant htt expression in cerebellar neurons (data not shown). Collectively, these results clearly deny the activation of HSF1 by mutant htt in granule cells. Although the results were unexpected, this conclusion matched well with the microarray result that other heat shock protein genes regulated by HSF1 were not changed in granule cells by mutant htt, except in the case of *hsp27* (Fig. 2, supplemental Tables 1, 2, available at www.jneurosci.org as supplemental material).

CBF and p53 are involved in the upregulation of *hsp70* in response to mutant htt

The gene expression of *hsp70* is also regulated by p53 (Agoff et al., 1993). p53 functions as a repressive cofactor to the transcription factor, CBF that upregulates *hsp70* via two CCAAT boxes in the promoter region (Agoff et al., 1993). We suspected that CBF and p53 might similarly regulate transcriptional activation in response to the mutant htt. We first examined the correlation whether CBF upregulates *hsp70* in HeLa cells by immunocytochemsitry (Fig. 7*B*). A positive relationship was clearly observed between CBF and *hsp70* expression, when the CBF-FLAG was transiently expressed in HeLa cells (Fig. 7*B*). In contrast, p53 signals generally tend to be low in aggregation-positive cells, especially in cells possessing perinuclear ring-like aggregates (supplemental Fig. 4, available at www.jneurosci.org as supplemental material). These results support our assumption that CBF and p53 regulate *hsp70*.

Next, using a CAT assay, we investigated whether CBF and

p53 directly regulate the *hsp70* gene in HeLa cells. Because *hsp70* was similarly upregulated in HeLa cells and granule cells in response to the mutant htt (Fig. 2), we analyzed transcriptional regulation with HeLa cells into which we can transfect plasmids more efficiently than into primary neurons. A CAT reporter plasmid containing the human *hsp70* gene promoter was first constructed and then multiple deletion plasmids lacking one or two CCAAT boxes were made from it (supplemental Fig. 5*A*, available at www.jneurosci.org as supplemental material). We performed CAT assays with these reporter plasmids in HeLa cells, and found that both of the two CCAAT boxes contributed to basal transcription of the *hsp70* promoter (supplemental Fig. 5*B*, available at www.jneurosci.org as supplemental material). In addition, the deletion of the two CCAAT boxes cancelled transactivation by mutant htt (supplemental Fig. 5*B*, available at www.jneurosci.org as supplemental material). Moreover, we confirmed that CBF and p53 regulated transcription of the human *hsp70* promoter in a positive and negative manner, respectively (supplemental Fig. 5*C*, available at www.jneurosci.org as supplemental material). The effects elicited by CBF and p53 were lost through the deletion of the CCAAT boxes from the promoter (data not shown). Collectively, the results of the CAT assay support the notion that CBF and p53 cooperatively regulate the gene expression of *hsp70* through the above-mentioned *cis*-elements.

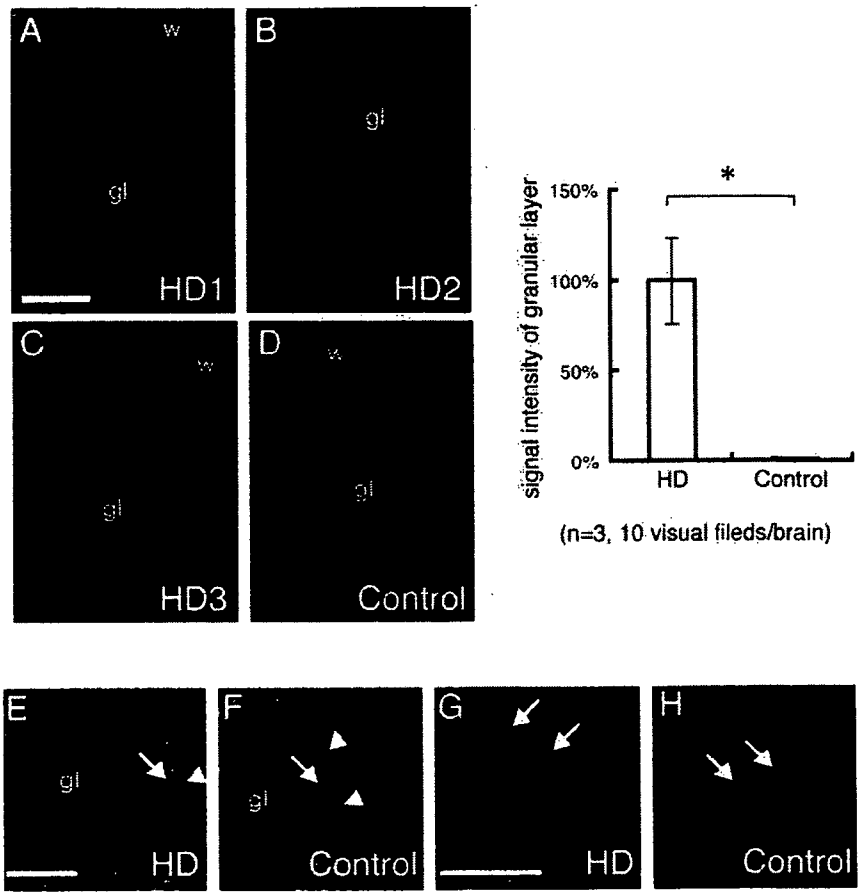

Figure 4. Hsp70 is increased in the cerebellar granule cells of human HD patients. ***A–C***, In the brains of HD patients, signal intensities of hsp70 are remarkably higher in the granular layer (gl) of the cerebellum than in white matter (w). ***D***, In contrast, the signal intensities of hsp70 of granular cell layers are lower than those of white matter in control brains. The right panel shows a comparison of the signal intensities in granular layers between HD and control brains. $^*p < 0.01$, Student's *t* test. ***E***, ***F***, High magnification confirmed the induction of hsp70 in the granule cells of the HD brain (gl in ***E*** vs ***F***). Meanwhile, Purkinje cells (***E*** and ***F***, arrows) show very low signals of hsp70 both in the HD and control brains (***E***, ***F***). Basket cells surrounding Purkinje cells show especially high signals (arrowheads). ***G***, ***H***, Signal intensities of hsp70 of the cortical neurons in the cerebral cortex (arrows) were closely similar between HD and the control. Scale bars: 10 μm. Error bars indicate SEM.

Basal expression and induction of p53 varies the response of *hsp70*

If this is the case, then why do cortical and cerebellar neurons show different effects on *hsp70* by the mutant htt? To answer the question, we performed CAT assays using primary cerebellar neurons (Fig. 8). Although transfection efficiency was very low, we could confirm in cerebellar neurons that CBF upregulated and p53 downregulated transcription through the *hsp70* gene promoter (Fig. 8*A*). Mutant htt stimulated transcription through the *hsp70* gene promoter (Fig. 8*A*, lane 1 vs 5). The effects of CBF and mutant htt were completely lost by deleting the CCAAT boxes from the promoter (Fig. 8*A*, lanes 4, 8) indicating that the transcriptional regulation was similar to that in HeLa cells. The coexpression of p53 repressed transactivation by CBF in granule cells (Fig. 8*B*). However, transfection of siRNA, although repressing p53, enhanced it slightly (Fig. 8*B*). In addition, we found in ChIP assays that mutant htt expression induced the binding of CBF to the *hsp70* gene promoter, both in cortical neurons and granule cells (Fig. 8*C*). Meanwhile, the attitude of p53 was different in cortical and in cerebellar neurons (Fig. 8*C*). p53 binds to the promoter in response to mutant htt expression in cortical neurons but not in cerebellar neurons (Fig. 8*C*). Furthermore, we confirmed that the siRNA-mediated suppression of CBF inhibited the mutant htt-induced upregulation of hsp70 (Fig. 8*D*). Collectively, these results suggest that the interaction of p53 to the transcription machinery on the *hsp70* gene promoter inhibits the expression of *hsp70* in cortical neurons, but the inhibition does not occur in cerebellar neurons.

To analyze the background of the different responses of p53 to mutant htt, we performed an immunocytochemical analysis with cerebellar and cortical neurons expressing the mutant htt (Fig. 9*A*). First, we found that the basal expression level of p53 was lower in cerebellar (CBL) neurons than in cortical (CTX) neurons (Fig. 9*A*, CBL-AxCA vs CTX-AxCA). In addition, most of the cerebellar neurons possessing inclusion bodies did not show the increase of p53. Only 2% of inclusion-positive cerebellar neurons showed an increase of p53 (p53-positive htt nuclear inclusion body) (Fig. 9), despite the fact that most of the p53 seemed to be sequestered into inclusion bodies. In contrast, in cortical neurons, p53 increased not only in inclusion body-positive cells, but also in inclusion body-negative cells (Fig. 9*A*, CTX). Western blotting with primary neurons also confirmed a far lower expression level of p53 in cerebellar neurons than in cortical neurons (Fig. 9*B*). In addition, Western blotting with mutant htt transgenic mice and age-matched control mice brains revealed a similarly low expression of p53 in the cerebellum (Fig. 9*C*). Interestingly, induction of p53 was also low in granule cells treated with

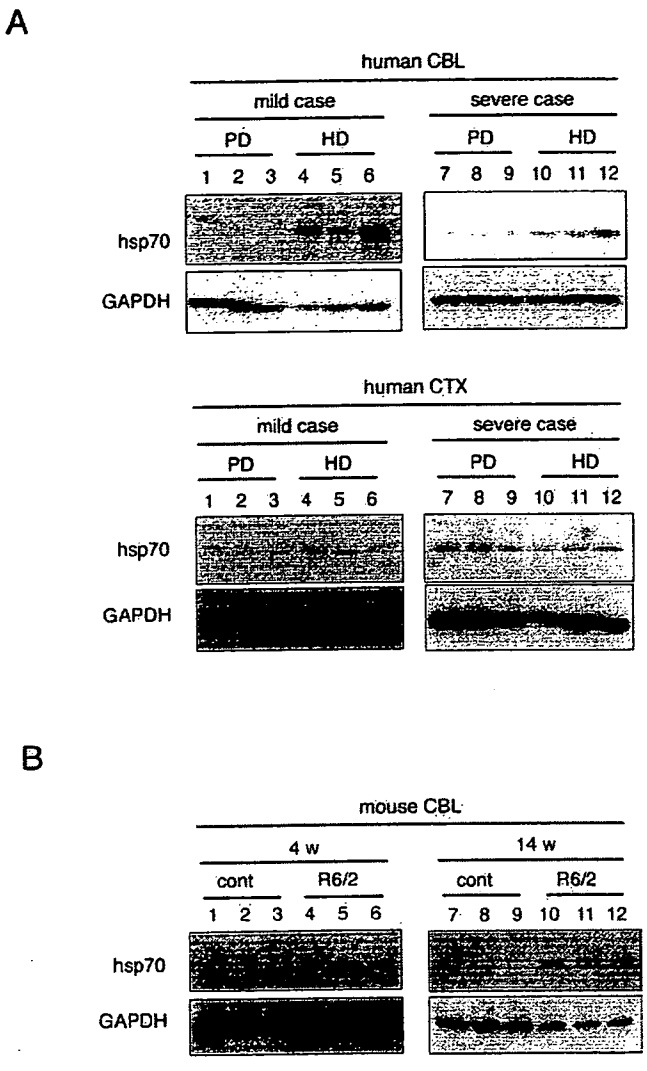

Figure 5. Western blot confirmation of the upregulation of hsp70 in the cerebellum of HD model mice and human HD patients. Western blotting performed with human HD brains (mild, grade 1–3; severe, grade 4, 5) and with PD brains (mild, Yahr's grade 1–3; severe, Yahr's grade 4, 5) confirmed HD-specific upregulation of hsp70 protein in the cerebellum. No upregulation was observed in the cerebral cortex (CTX). For the Western blots, surface tissues (1 mm thick) were prepared under the microscope from the cerebellar hemisphere cortex (CBL) or the prefrontal lobe cortex (CTX) that had been preserved at −80°C after autopsy. Western blotting was performed with R6/2 mutant htt-transgenic mice at different ages. The upregulation of hsp70 was observed in the cerebellum of both the presymptomatic mice [4 weeks (w)] and symptomatic mice (14 w).

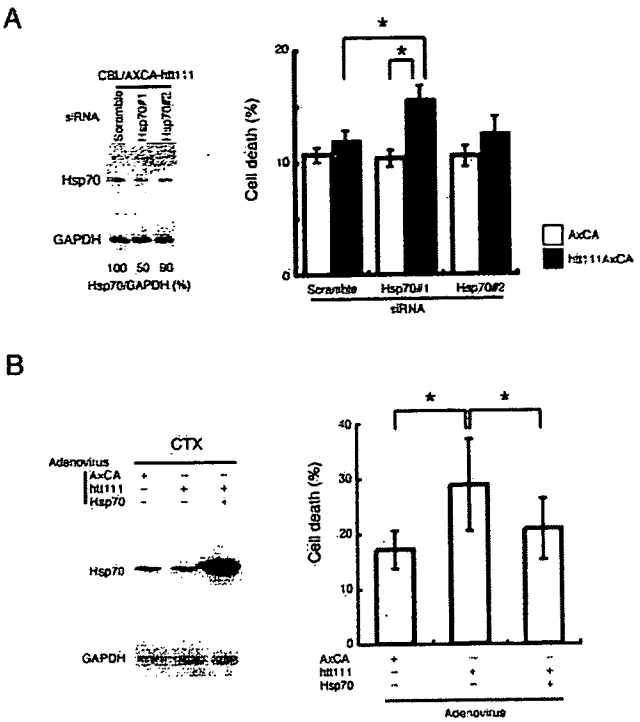

Figure 6. The expression levels of *hsp70* affect the vulnerability of primary neurons to mutant htt. ***A***, When *hsp70* upregulation by mutant htt is diminished by siRNA, granule cells become vulnerable to mutant htt. $^*p < 0.01$, Student's *t* test. Two types of siRNA (Hsp70#1, Hsp70#2) were transfected into in cerebellar neurons to repress upregulation of *hsp70* by mutant htt. Hsp70#1 reduced *hsp70* up to 50% (the effect was limited because of a low transfection efficiency of primary neurons with lipofection), whereas Hsp70#2 was not effective. ***B***, Coexpression of *hsp70* with mutant htt in cortical neurons reduced cell death when compared with the single expression of mutant htt ($^*p < 0.01$, Student's *t* test). Independent experiments were performed 20 times. Error bars indicate SEM.

bleomycin (supplemental Fig. 6, available at www.jneurosci.org as supplemental material), thus suggesting that the insensitivity of p53 is a characteristic of granule cells.

The interaction of p53 with mutant htt has been reported previously by other researchers (Steffan et al., 2000; Bae et al., 2005). The interaction by itself and/or resultant sequestration into inclusion bodies may repress the transcriptional activity of p53. We have reported previously that the aggregation manners of mutant htt are different among neuronal subtypes (Tagawa et al., 2004). Mutant htt forms various inclusion bodies in the morphology, and nuclear inclusion bodies increase chronologically in all neuronal subtypes. The frequency of each type of inclusion body and the ratio of nuclear inclusion bodies are clearly different among neurons (Tagawa et al., 2004). In granule cells, nuclear inclusions emerge more promptly and more frequently than in other types of neurons (Tagawa et al., 2004). The prompt formation of nuclear inclusions in granule cells might be thus considered to inactivate p53 more than in other neurons. To support this idea, we found that the ratio of mutant htt-induced cell death was lower in p53 aggregation-positive cortical neurons than in aggregation-negative (diffusely stained) cortical neurons (supplemental Fig. 7, available at www.jneurosci.org as supplemental material).

To summarize the results of the promoter assays and the immunohistochemical analyses, different levels of p53 under mutant htt expression may explain the different responses of *hsp70* observed in cortical and cerebellar neurons (Fig. 10).

Discussion

A novel mechanism underlying neuron subtype-selective pathology

This study originated with our question into why specific subtypes of neurons are vulnerable in neurodegenerative disorders, and why such vulnerable subtypes are different in various disorders. To answer these questions, we performed microarray analyses of three types of primary neurons expressing normal/mutant htt or Atx-1, and found that *hsp70* regulated neuron subtype-specific vulnerability in the HD pathology. Looking at changes in expression, we found selective upregulation of *hsp70* in cerebellar neurons by mutant htt. The upregulation was induced in neither

of the other neuronal subtypes by mutant htt, nor in granule cells by mutant Atx-1. This indicates that upregulation is highly specific to the expression of mutant htt in granule cells. Although a certain culturing condition might affect the expression levels of *hsp70*, we repeated the primary culture of neurons >30 times for both the microarray and Western blot analyses and the results were highly reproducible. Furthermore, other heat shock factors such as hsp40, hsp84, hsp105α, and MRJ were not changed in our microarray and Western blot analyses (data not shown), ruling out the possibility that a certain stress during the culture caused upregulation of *hsp70*.

Therefore, the selective upregulation of *hsp70* could be a novel mechanism underlying the selective neurodegeneration, distinct from the mechanisms reported previously (Waragai et al., 1999; Li et al., 2000; Humbert et al., 2002; Okazawa et al., 2002; Rangone et al., 2004; Warby et al., 2005). It is of note that all of these mechanisms reported previously accelerate the pathology, and no protective factor has been implicated in the selective pathology. Therefore, this study constitutes the first research to suggest the novel concept that neuroprotective factor(s) might also be involved in neuronal subtype-selective pathology.

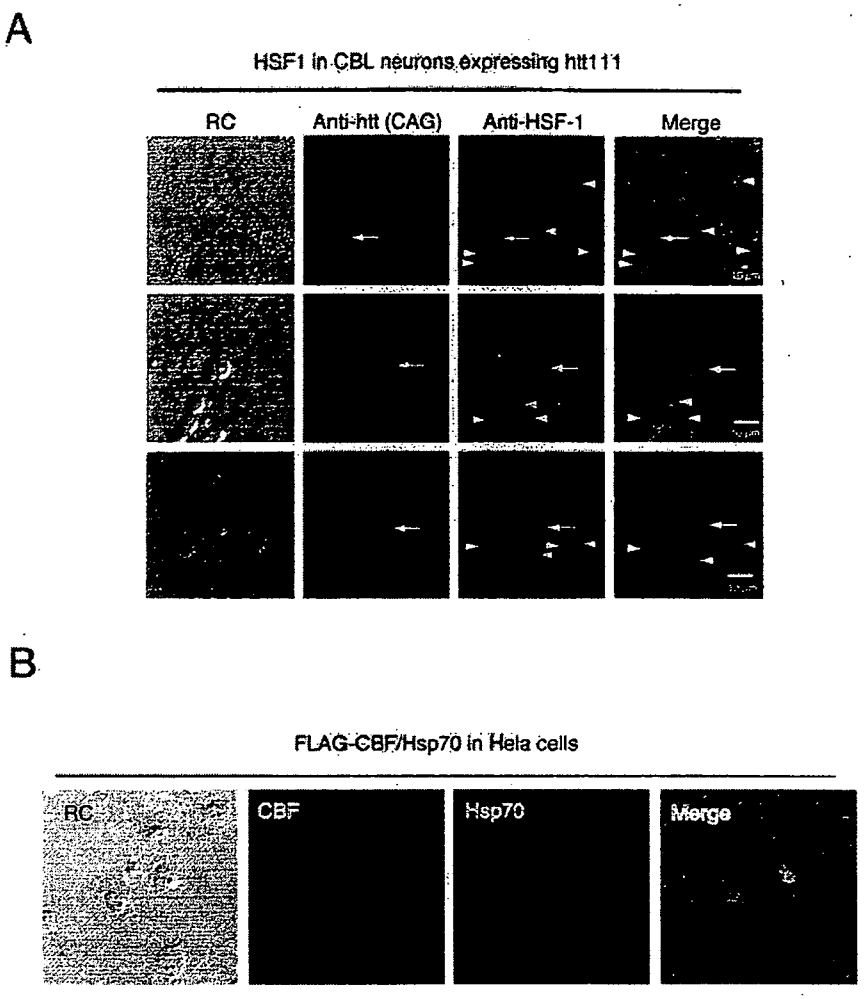

Figure 7. HSF1 is not activated by the expression of mutant htt. *A*, Immunohistochemistry revealed that HSF1 was not increased in cerebellar neurons expressing mutant htt. The signal intensities of HSF1 were similar in neurons expressing mutant htt (arrows) and in neurons without the immunostaining of mutant htt (arrowheads). Notably, HSF1 remained in the cytoplasm of mutant htt-expressing neurons, and no translocation of HSF1 to the nucleus was observed. *B*, CBF induces expression of hsp70. Transiently expressed FLAG-CBF was detected by an anti-FLAG antibody. The anti-hsp70 (K20) antibody detected induction of hsp70 in HeLa cells overexpressing CBF. RC, Relief contrast.

P53 regulates transcriptional induction of *hsp70* in cerebellar neurons

Unexpectedly, our results exclude the possibility that HSF1 upregulates *hsp70* in cerebellar neurons expressing mutant htt. Retrospectively, however, these results seem natural, as HSF1-regulated heat shock proteins such as hsp40, hsp84, hsp105α, and MRJ were not changed in our microarray and immunoblot analyses (data not shown). Instead, we found that p53, which represses transactivation by CBF as a negative cofactor (Agoff et al., 1993), regulates *hsp70* in cerebellar neurons.

Both in HeLa cells and in primary cerebellar neurons, CBF activated and p53 repressed transcription of the *hsp70* gene (Fig. 7*B*, 8). CBF bound to the promoter in response to the expression of mutant htt (Fig. 8). In cortical neurons, basal and mutant htt-induced expression levels of p53 were high, whereas the levels of p53 were low in cerebellar neurons. Therefore, induction of *hsp70* by CBF is not disturbed by p53 in cerebellar neurons (Fig. 10).

Various studies have suggested the involvement of p53 family proteins in the polyQ pathology (Hoshino et al., 2006). p53 mediates cellular dysfunction and behavioral abnormalities in HD animal models (Bae et al., 2005). p53 binds to the upstream and intron regions of the human *htt* gene and upregulates the gene expression of *htt* in cortical and striatal neurons (Feng et al., 2006). These findings suggest the direct toxic roles of p53 in the HD the pathology. In contrast, our study shows the indirect role of p53 to inhibit the cell-protective response of *hsp70* at the transcription level (supplemental Fig. 8, available at www.jneurosci.org as supplemental material). The indirect role of p53 also seems consistent with the protective function of inclusion bodies (Arrasate et al., 2004; Tagawa et al., 2004), considering the sequestration of p53 into the inclusion bodies (Steffan et al., 2000).

Relationship among mutant htt, hsp70, and p53 in the pathology

Mutant polyQ proteins seem to induce the conformational change of a wide range of proteins and thereby affect the physiological metabolism of neurons (Gidalevitz et al., 2006). Hsp70 could antagonize such a general effect on cellular proteins. Actually, a number of studies support the concept that *hsp70* protects neurons in the polyQ pathology (Cummings et al., 1998, 2001; Chai et al., 1999; Warrick et al., 1999; Zhou et al., 2001; Adachi et al., 2003), and the Muchowski group previously revealed that *hsp70* partitions monomers of mutant huntingtin to prevent the formation of spherical or annular oligomers (Wacker et al., 2004). Therefore, the upregulation of *hsp70* in the nuclei of granule cells is considered to reduce the toxicity of mutant htt oligomers and to recover the physiological functions of various nuclear proteins.

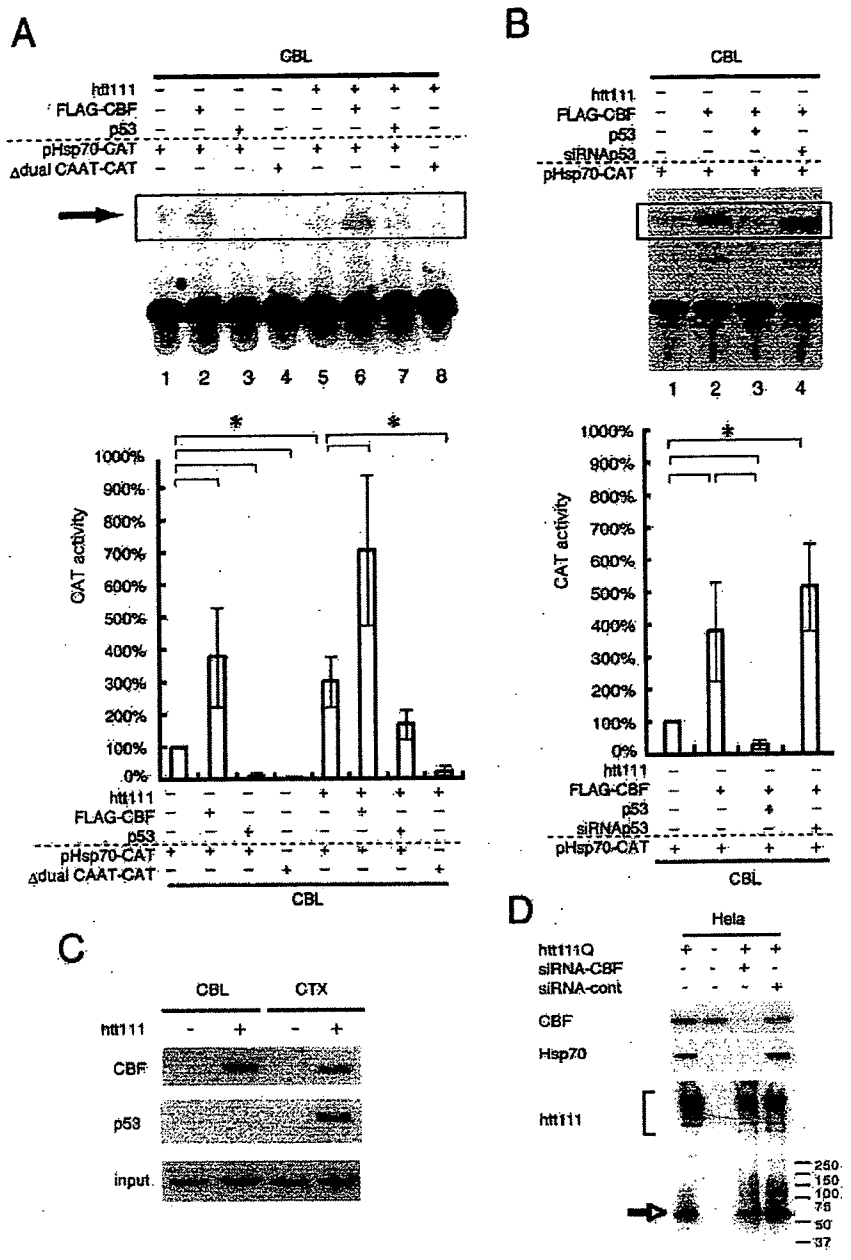

Figure 8. Mutant htt regulates the expression of *hsp70* in cerebellar neurons through CBF and CCAAT boxes. ***A***, Basal transcription from the *hsp70* promoter was increased to threefold by expression of mutant htt (lane 1 vs 5). CBF additionally enhances transcription (lanes 2, 6) whereas p53 represses basal transcription (lanes 3, 7). The effects of exogenously expressed CBF and p53 were similar regardless of mutant htt (lanes 1–3, 5–7). When the two CCAAT boxes were deleted, transcriptional activation of the *hsp70* gene promoter was completely lost (lane 8), indicating that mutant htt upregulates *hsp70* gene expression through the two CCAAT boxes. The lower graph shows a quantitative analysis of CAT activities. Asterisks indicate statistically significant differences according to Student's *t* test ($p < 0.05$). ***B***, p53 expression levels critically affect transactivation by CBF through the *hsp70* promoter. The coexpression of p53 represses transactivation by CBF, whereas reduction of p53 with siRNA enhances transactivation by CBF. Asterisks indicates statistically significant differences according to Student's *t* test ($p < 0.05$). ***C***, The ChIP assay shows that mutant htt induces the interaction of CBF with the *hsp70* promoter. p53 binds to the promoter only in cortical neurons expressing mutant htt. Although p53 is expressed in primary cortical neurons in the absence of mutant htt (Fig. 9), p53 does not bind to the promoter. This means that the binding of p53 to the *hsp70* gene promoter depends on CBF because the promoter possesses no p53 binding consensus sequence. ***D***, The mutant htt-induced upregulation of hsp70 was repressed in HeLa cells by cotransfection of CBF-specific siRNA but not by nonspecific siRNA. The effect of siRNA on the CBF protein levels was assayed with coexpressed FLAG-CBF by the transfection of pCI-FLAG-CBF. Error bars indicate SEM.

This study shows that p53 negatively regulates *hsp70* gene expression as a repressive cotranscription factor of CBF (Fig. 8). Meanwhile, *hsp70* is known to inactivate p53 by dissociating the p53 tetramer in the nucleus and by participating in the cytoplasmic sequestration or degradation of p53 (Zylicz et al., 2001). Therefore, hsp70 and p53 seem to form a negative-feedback loop, suppressing each other. However, Feng et al. (2006) reported induction of *htt* by p53. Bae et al. (2005) and the present study have shown induction of p53 by mutant htt. Thus, htt and p53 seem to constitute a positive-feedback loop. The expression levels of p53 might classify neurons into a vulnerable group or a resistant group through the two functionally opposite feedback loops (supplemental Fig. 8, available at www.jneurosci.org as supplemental material).

Other candidate genes in the polyQ pathologies

In microarray analyses, we found some other genes that may be relevant to the polyQ pathologies (Fig. 1*B*), although we did not investigate them in this study. Such genes include *Omi*, *Cbl-2*, and *RoXaN*, which are downregulated in striatal neurons specifically by mutant htt. Omi is a mitochondrial serine protease normally present in the intermembrane space of mitochondria, whose mutation has been shown to cause degeneration of striatal neurons and motor neurons (Jones et al., 2003). The mutation seems to activate mitochondrial permeability transition pores and make neurons vulnerable to proapoptotic agents (Jones et al., 2003). Furthermore, *Omi* mutations are suggested to link to sporadic Parkinson's disease (Strauss et al., 2005), whereas patients of familial PD (PARK3) did not carry any mutation in exons or around splicing junctions (Jones et al., 2003). Therefore, *Omi* could be a candidate gene involved in the polyQ pathology. Cbl-b is an E3 ubiquitin ligase that mono-ubiquitinates membrane receptors for recycling through clathrin vesicles. It is important to note that HIP1 (huntingtin interacting protein 1) is involved in the submembrane molecular structure of clathrin-coated vesicles (Engqvist-Goldstein et al., 1999; Kim et al., 1999; Metzler et al., 2001; Rao et al., 2001; Waelter et al., 2001a,b; Legendre-Guillemin et al., 2005). The substrates of Cbl-b include the epidermal growth factor receptor, colony-stimulating factor 1 receptor, hepatocyte growth factor receptor/Met, and so on (Peschard and Park, 2003). The third gene, *RoXaN*, which is downregulated by mutant htt in striatal neurons, is a novel cellular protein that forms a ternary complex with the initiation factor 4G and rotavirus protein neuroendocrine-specific protein 3 (Vitour et al., 2004). However, the physiological functions of *RoXaN* remain mostly unknown. The pathophysiological function of hnRNPH, which is upregulated in resistant neurons in two polyQ pathologies,

should also be analyzed. Our group is currently investigating the pathological functions of these candidate molecules by expressing them in primary neurons with mutant polyQ proteins (Inagaki, Qi, and Okazawa, unpublished observation).

A comparison with other studies of gene expression profiling in HD models

Several groups have reported a transcriptome analysis of the HD pathology. Luthi-Carter et al. (2002a,b) analyzed two types of HD model mice (R6/2 and N171–82Q) with gene chips and found that multiple genes in various signaling pathways are diminished in both models. Chan et al. (2002) compared gene expression profiles among four transgenic mice expressing short peptides or the full-length protein of mutant htt, and reported their expression profiles to be different. Strand et al. (2005) applied this technique to skeletal muscle samples of HD patients to search for biomarkers. Sipione et al. (2002) investigated early the transcriptional profiles in huntingtin-inducible striatal cells. The results from these experiments, however, are not completely consistent, suggesting that microarray results, even from repeated experiments, could be modified by various experimental conditions and therefore should be considered as initial data presenting candidate genes, but not genuine pathological participants.

Previously, Hodges et al. (2006) reported a microarray analysis of multiple brain regions of human HD patients. The genes selected on the basis of expression were mostly different between their study and our own. Several reasons may explain the differences. First, their group used human brains containing a large number of glial cells and vascular cells, whereas our primary culture contained <1% of astrocytes and no vascular cells. Second, we were able to prepare mRNA at the starting point of inclusion body formation, whereas their analysis was performed on patients at the age of >40 years. Most patients were already symptomatic, suggesting their brain tissue already contained numerous inclusions. However, our study could receive the criticism that primary neurons *in vitro* might have different characters from those of neurons *in vivo*. However, as we have already discussed, the array should be considered as an initial tool to approach candidates, and confirmation or selection of the candidates is more important. Hence, this study shows that *hsp70* is indeed changed in patients' brains *in vivo* and that the protective function of *hsp70* has been well established even beyond to our present results. Therefore, it is highly plausible that cerebellar neuron-specific upregulation of *hsp70* contributes to selective pathologies in HD. Finally, data from multiple studies should be integrated to uncover the true pathological transcriptome, because the basic idea is common among the various studies.

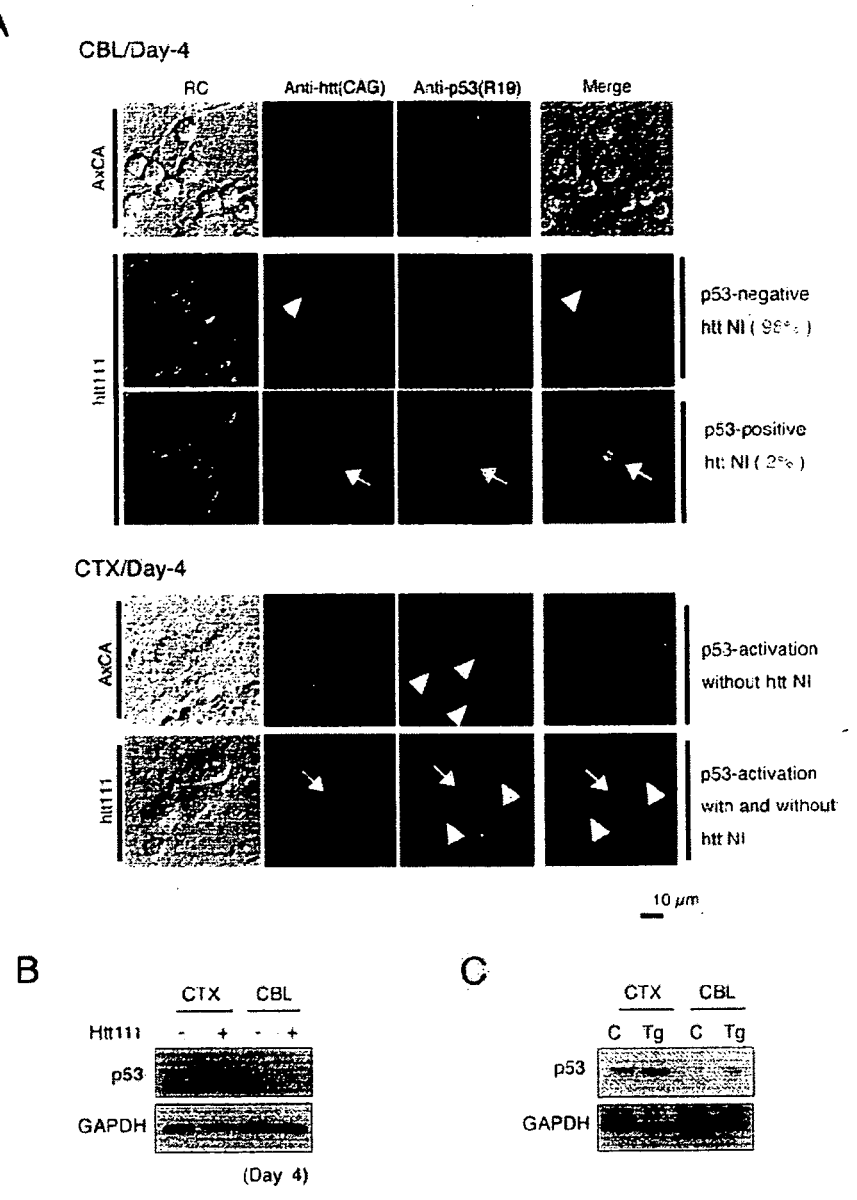

Figure 9. The response of p53 is clearly different in granule cells and cortical neurons. *A*, The basal level expression of p53 is higher in cortical neurons (CTX, AxCX) than in granule cells (CBL, AxCA). The expression of mutant htt does not upregulate p53 in most of mutant htt-expressing granule cells (CBL, arrowhead). In addition, the inclusion bodies of mutant htt sequestered p53 are upregulated in only a small part of granule cells (CBL, arrows). In contrast, most p53 is not sequestered into inclusion bodies in cortical neurons (CTX, arrowhead). To calculate the percentages of p53-positive and -negative granule cells, >100 inclusion body-positive cells were counted in primary cerebellar neuron. Nuclear inclusion bodies were detected by the CAG53b antibody in 2% of cerebellar granule cells (top panels), whereas they were very rare among cortical neurons (bottom panels). It is important to note that inclusion-body formation did not affect p53 foci formation (arrow). Mutant htt was expressed in cerebellar and cortical neurons by adenovirus vectors (AxCA, htt(exon1)111Q), as described in Materials and Methods. *B*, Western blotting with primary neurons confirmed that the expression level of p53 to be far lower in the cerebellar neurons (CBL) than in the cortical neurons (CTX). *C*, Western blotting with 4-week-old mutant htt transgenic (Tg) and age-matched control (C) mouse brain showed p53 to be similarly lower in the cerebellum than in the cerebral cortex.

Conclusion

In this study, we identified the novel phenomenon that *hsp70* is upregulated specifically in cerebellar granule cells. In addition, our findings show that the underlying mechanism might be a neuron